Supplementary Figure 1

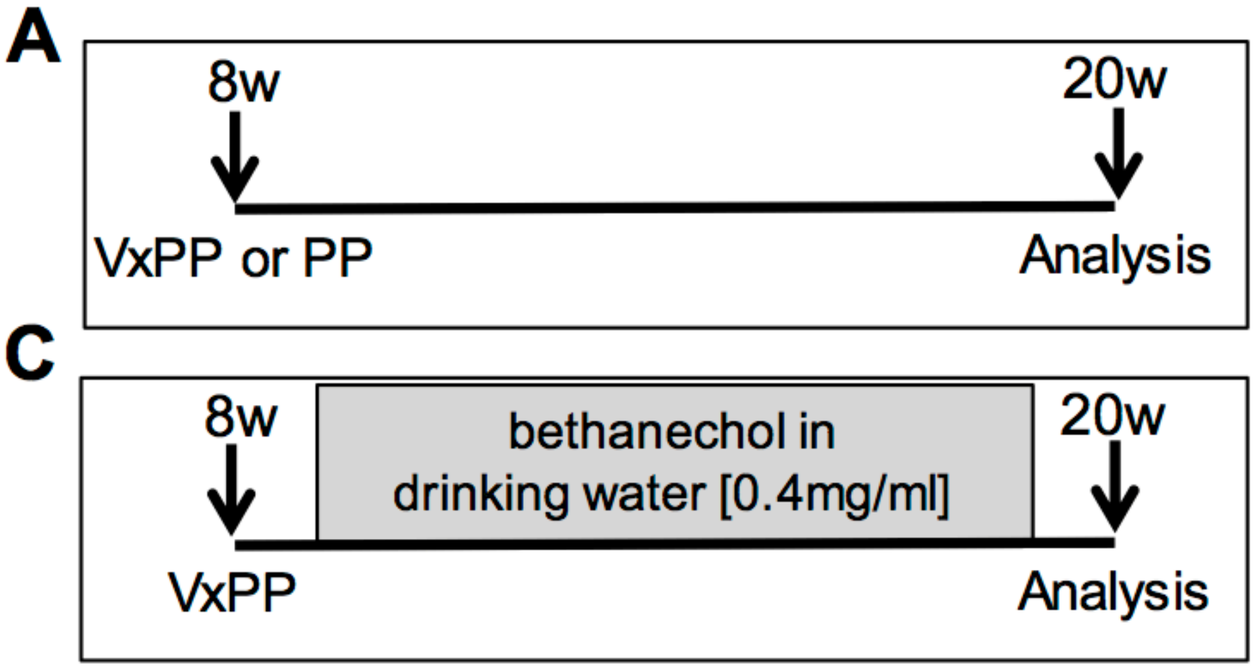

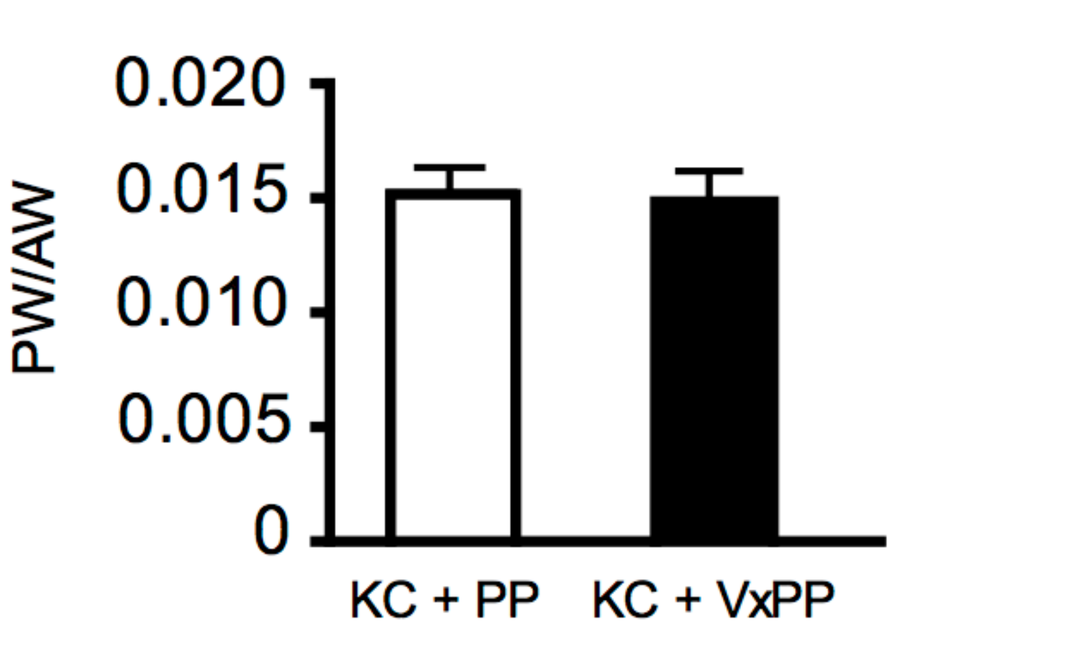

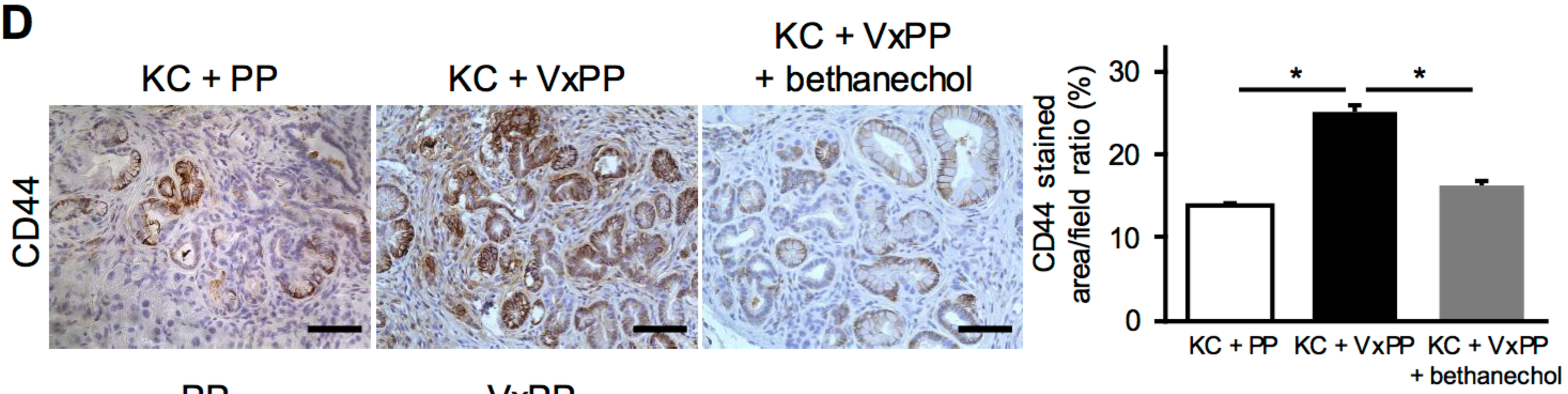

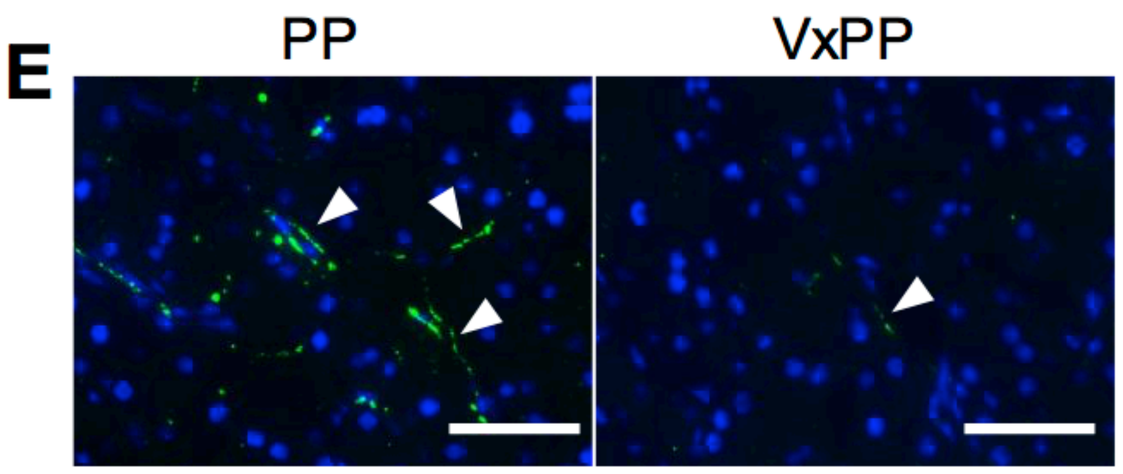

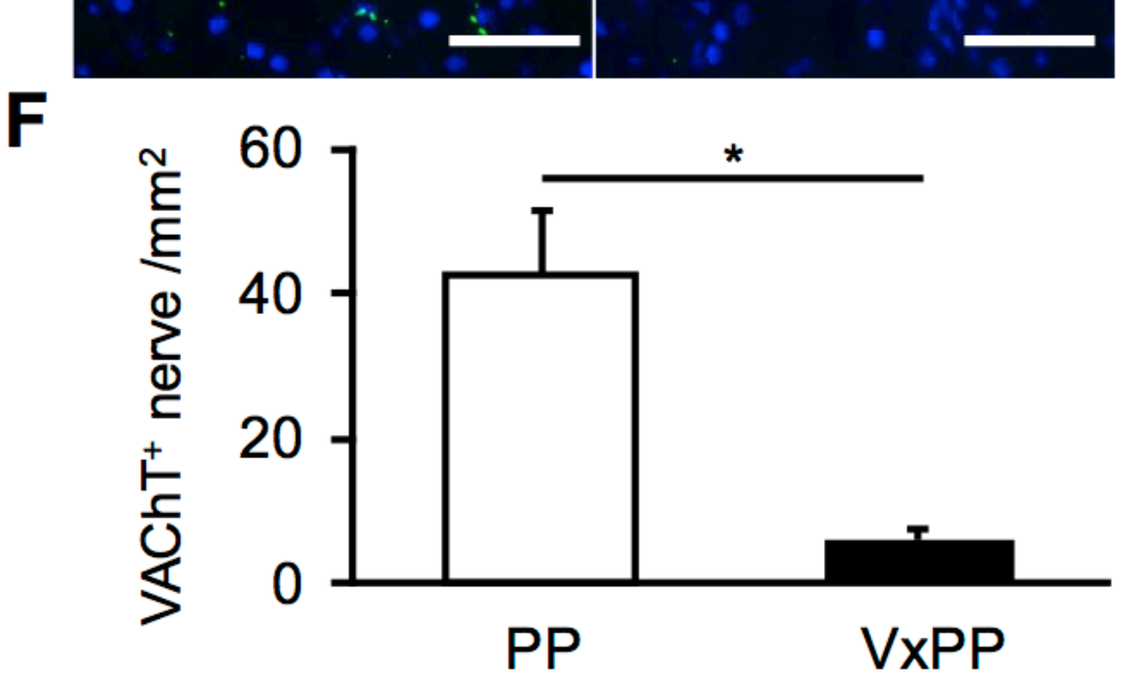

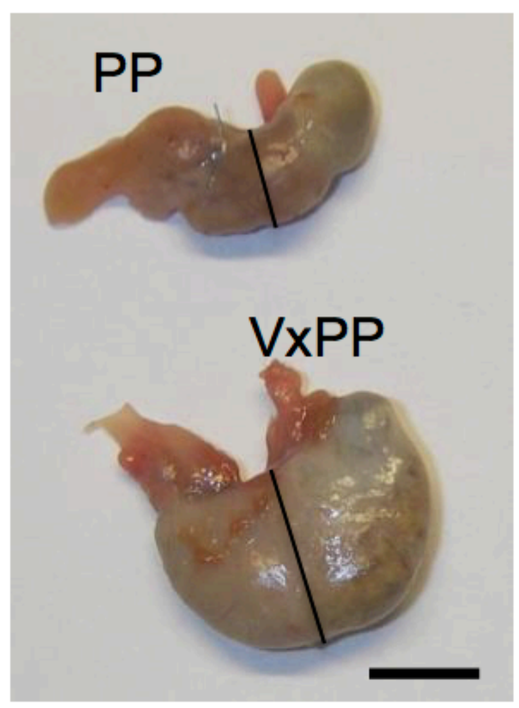

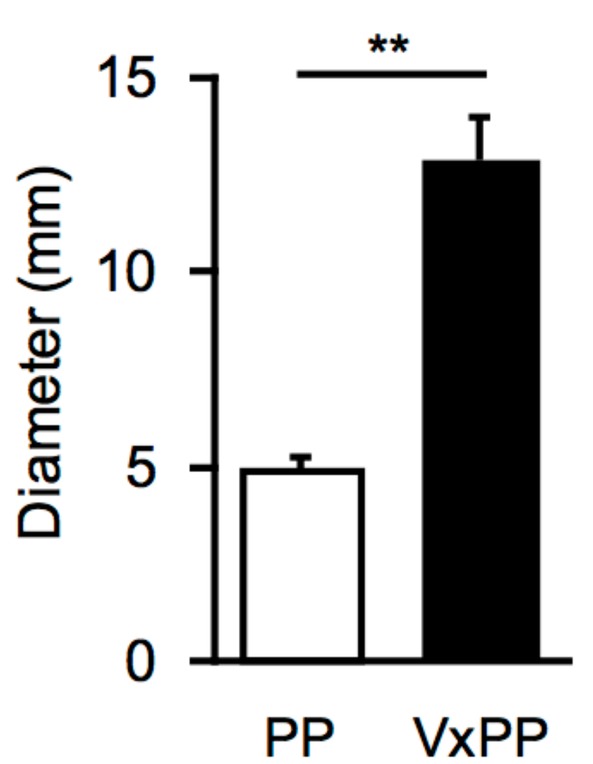

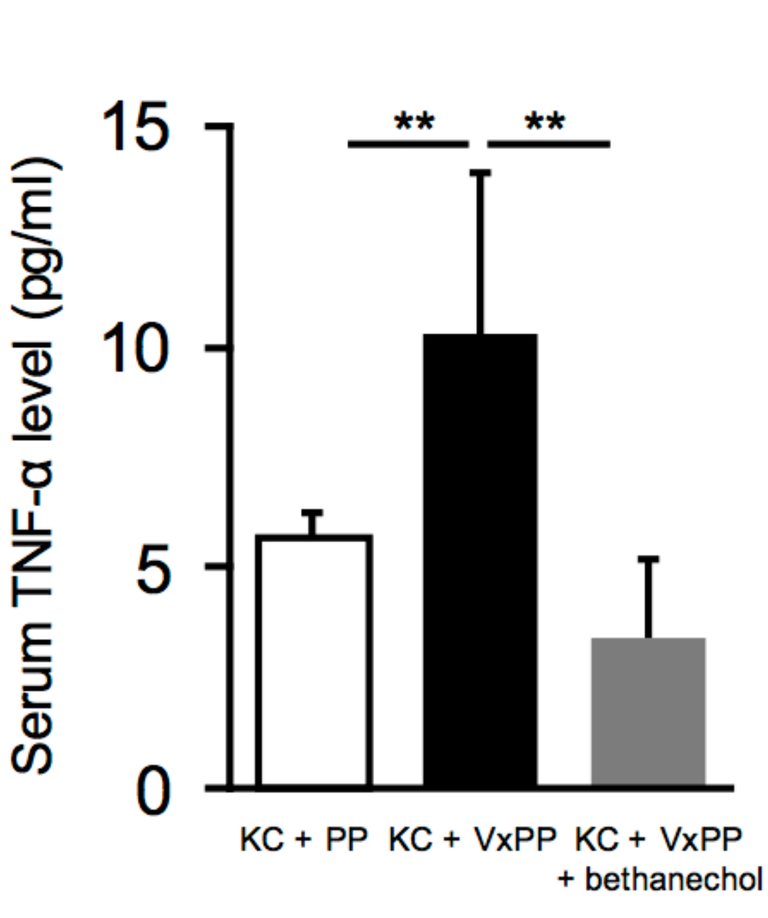

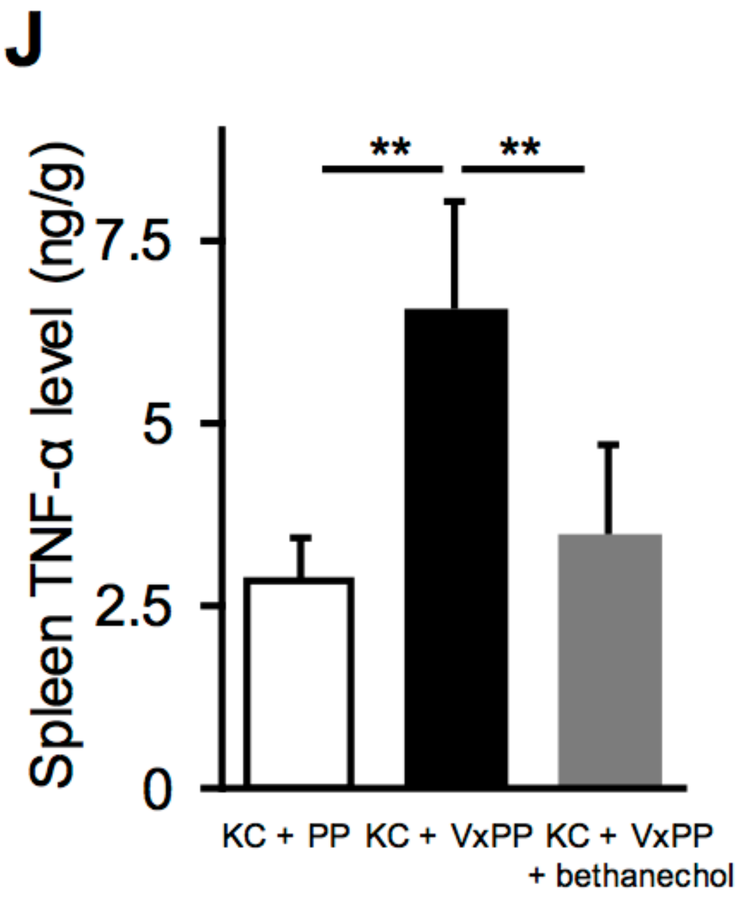

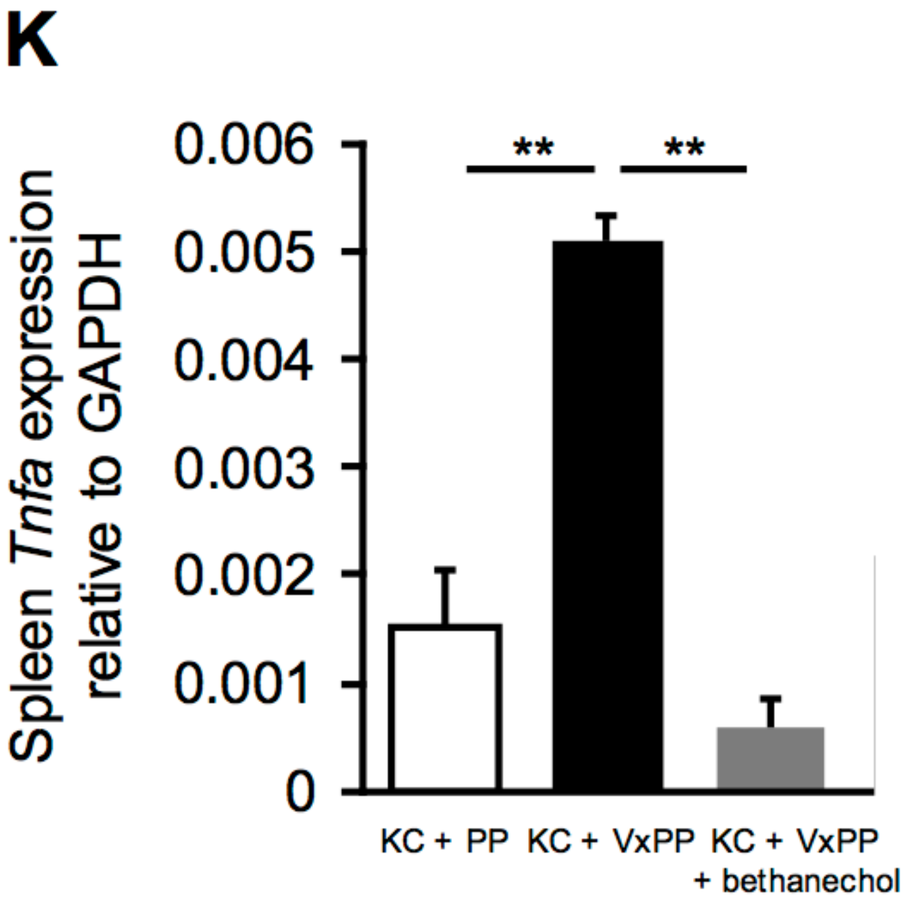

Supplementary Figure 1 (cont'd)

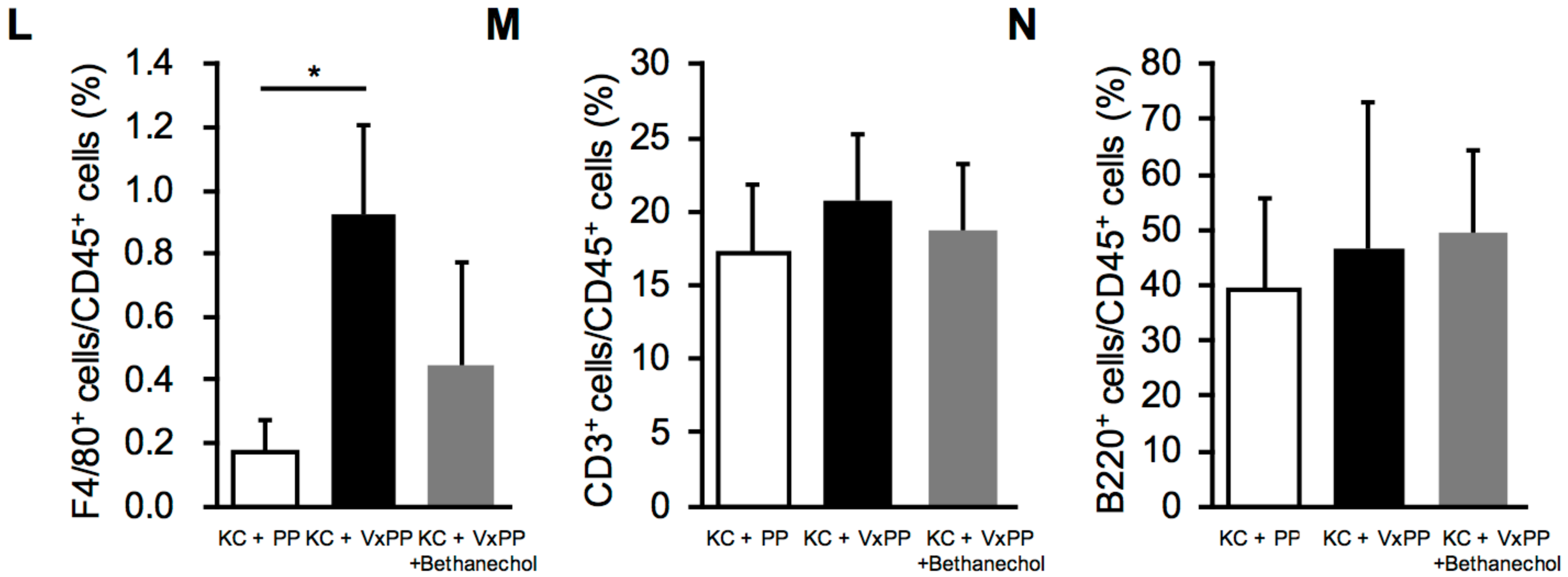

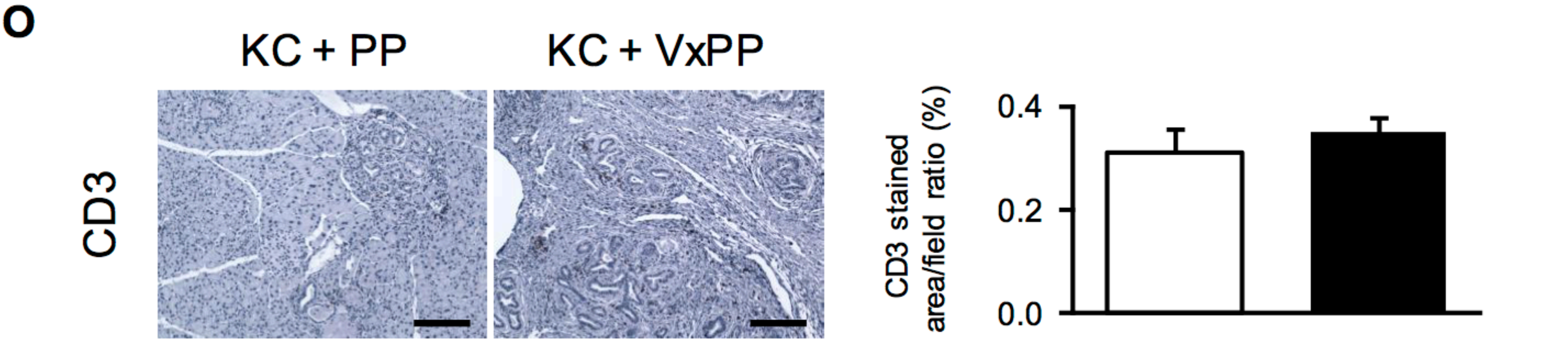

Supplementary Figure 1

A. Experimental setup: KC mice were randomized to undergo VxPP (n=12) or PP (n=10), which were performed at 8 weeks after birth. Mice were sacrificed and analyzed at 20 weeks. **B.** Pancreatic weight/body weight ratio (PW/BW) in KC+PP mice compared to KC+VxPP mice. **C.** Experimental setup: KC mice underwent VxPP at 8 weeks and were subsequently treated with bethanechol in the drinking water (400 μg/ml) (KC+VxPP + bethanechol) (n=13) or water without bethanechol (n=12). Mice were sacrificed and analyzed at 20 weeks. **D.** Representative images of pancreatic IHC for CD44 in KC+PP, KC+VxPP and KC+VxPP+bethanechol mice at 20 weeks. Bar graph showing quantification of CD44 stained area in pancreata from KC+PP, KC+VxPP and KC+VxPP+bethanechol mice (n = 3, each group); Scale bars, 100 μM. **E.** Representative images of pancreatic immunofluorescent staining for VAChT in WT +PP and WT+VxPP mice (VAChT; green, DAPI; blue). White arrowheads indicate $VAChT^+$ nerve. Scale Bar, 50 μm. **F.** Bar graph showing quantification of $VAChT^+$ nerve number in pancreata from WT + PP and WT + VxPP mice at 20 weeks (n=3, each group); Scale bars, 50 μm. **G.** Representative photograph shows stomachs of KC+PP (PP) and KC+VxPP (VxPP) mice at 16 weeks. Black bars indicate the diameter of the stomach (Scale bar; 5 mm). **H.** Bar graph comparing diameter of stomachs of KC +PP(PP) and KC+VxPP (VxPP) mice at 20 weeks. **I.** Serum TNF-α levels from KC+PP, KC+VxPP and KC+VxPP+bethanechol mice measured by ELISA at 16 weeks (n=3/per group) **J.** Splenic TNF-α levels from KC+PP, KC+VxPP and KC+VxPP+bethanechol mice measured by ELISA at 16 weeks (n=3/per group). **K.** Relative quantification of mRNA expression of splenic TNF-α expression in KC+PP, KC+VxPP and KC+VxPP+bethanechol mice (n=3/per group). **L-N.** Bar graphs showing quantification of splenic $F4/80^+$ (**L**), $CD3^+$ (**M**), and $B220^+$ (**N**) cells among all $CD45^+$ cells in KC+PP, KC+VxPP and KC+VxPP + bethanechol mice at 16 weeks (n=3/per group). **O-S.** Representative images of pancreatic IHC for CD3 (**O**), B220 (**P**), αSMA (**Q**), CgA (**R**), and CD31 (**S**) in KC+PP and KC+VxPP mice at 20 weeks. Bar graphs show quantification of stained area in pancreata from KC+PP and KC+VxPP mice at 20 weeks (n= 4, each group); Scale bars, 100 μM. Means ± SD. *$p < 0.05$; **$p < 0.01$.

Supplementary Figure 2

A

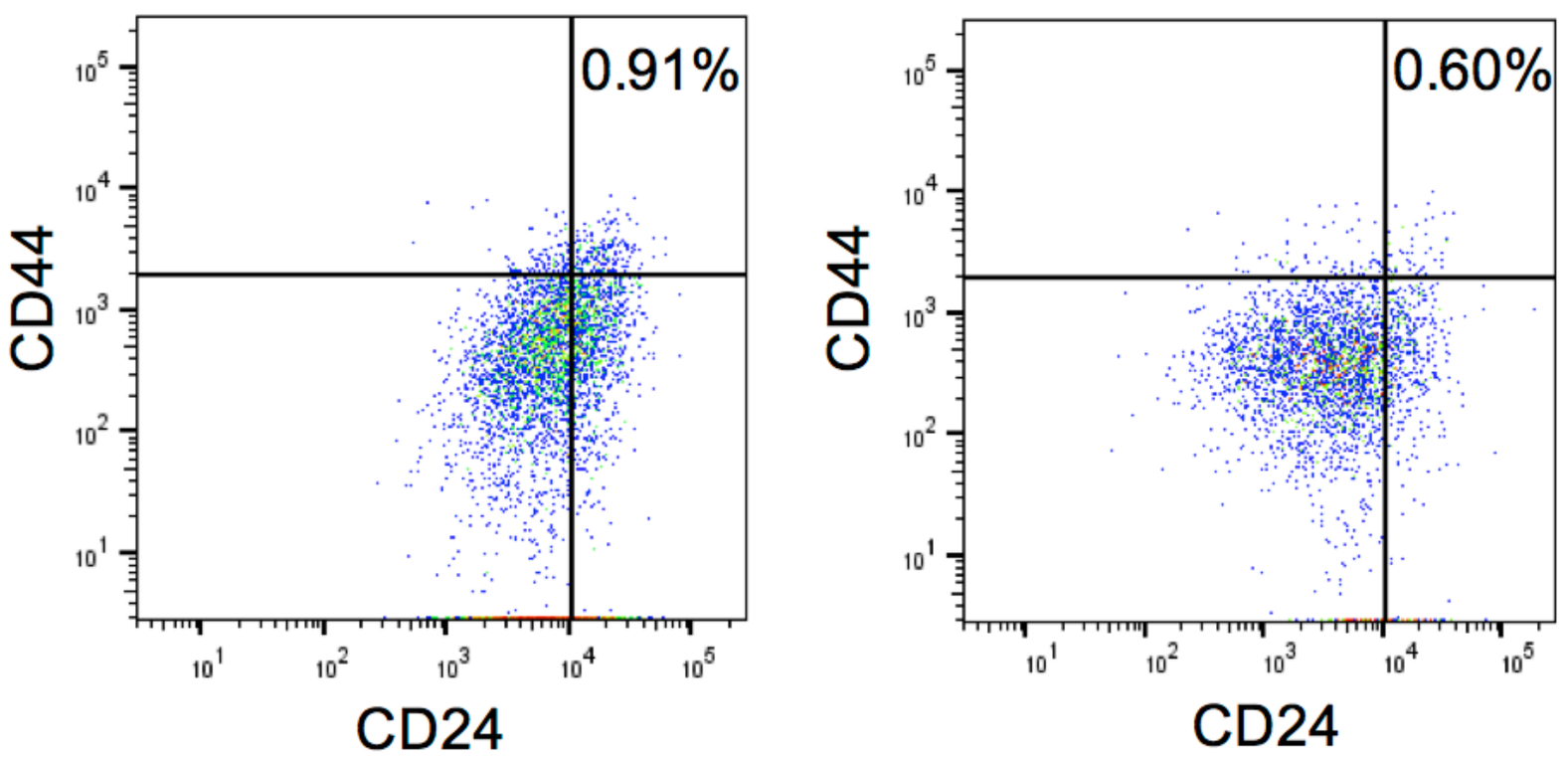

B

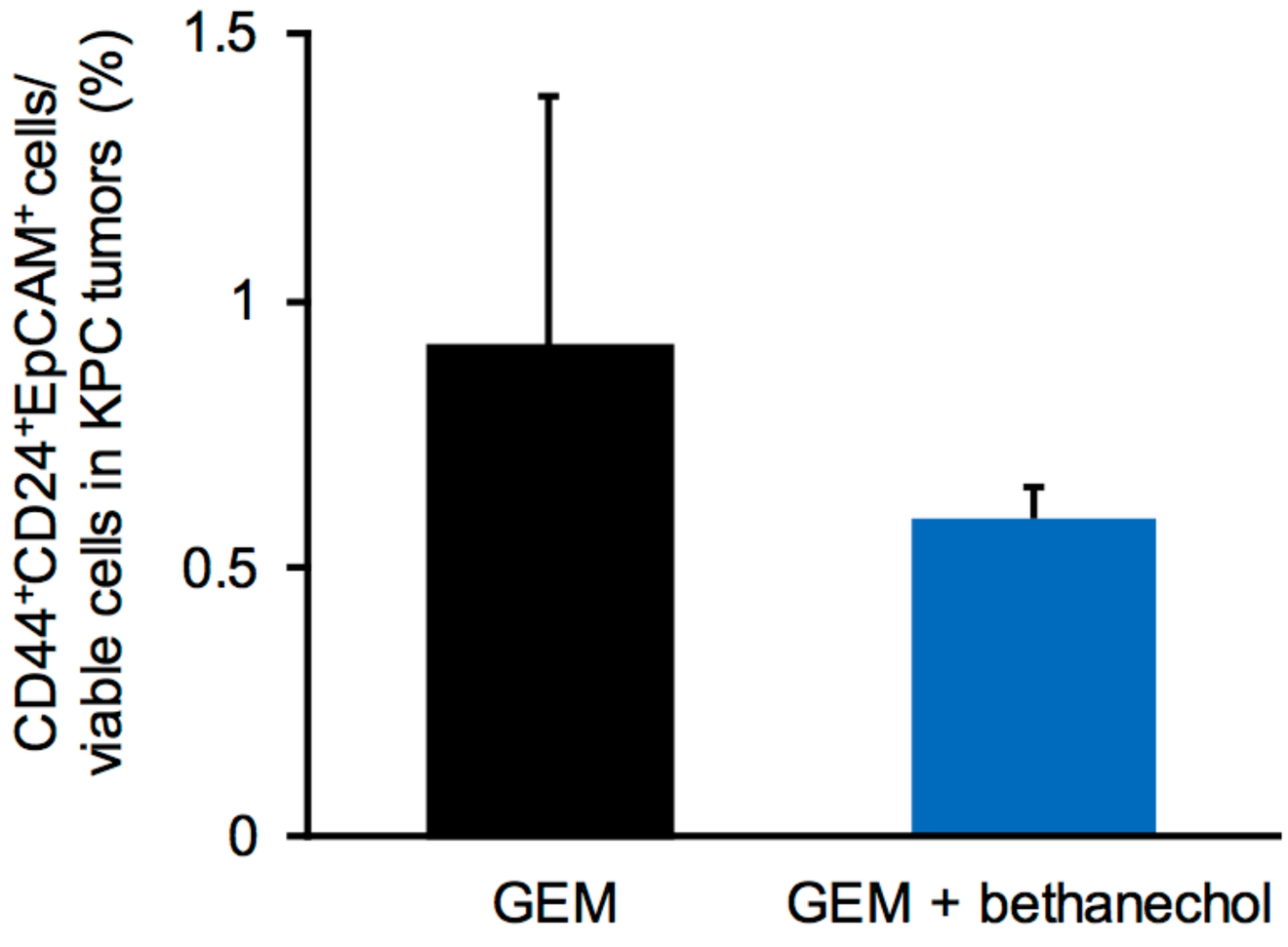

Supplementary Figure 2

A. Representative flow cytometric plot analysis of $CD44^+CD24^+EpCAM^+$ cells in PDAC from KPC mice treated with GEM or GEM+bethanechol. The numbers are showing the ratio of $CD44^+CD24^+EpCAM^+$ cells to viable cell number. **B.** Bar graph showing quantification of $CD44^+CD24^+EpCAM^+$ cells in PDAC from KPC mice treated with GEM (n=3) or GEM+bethanechol (n=4).

Supplementary Figure 3

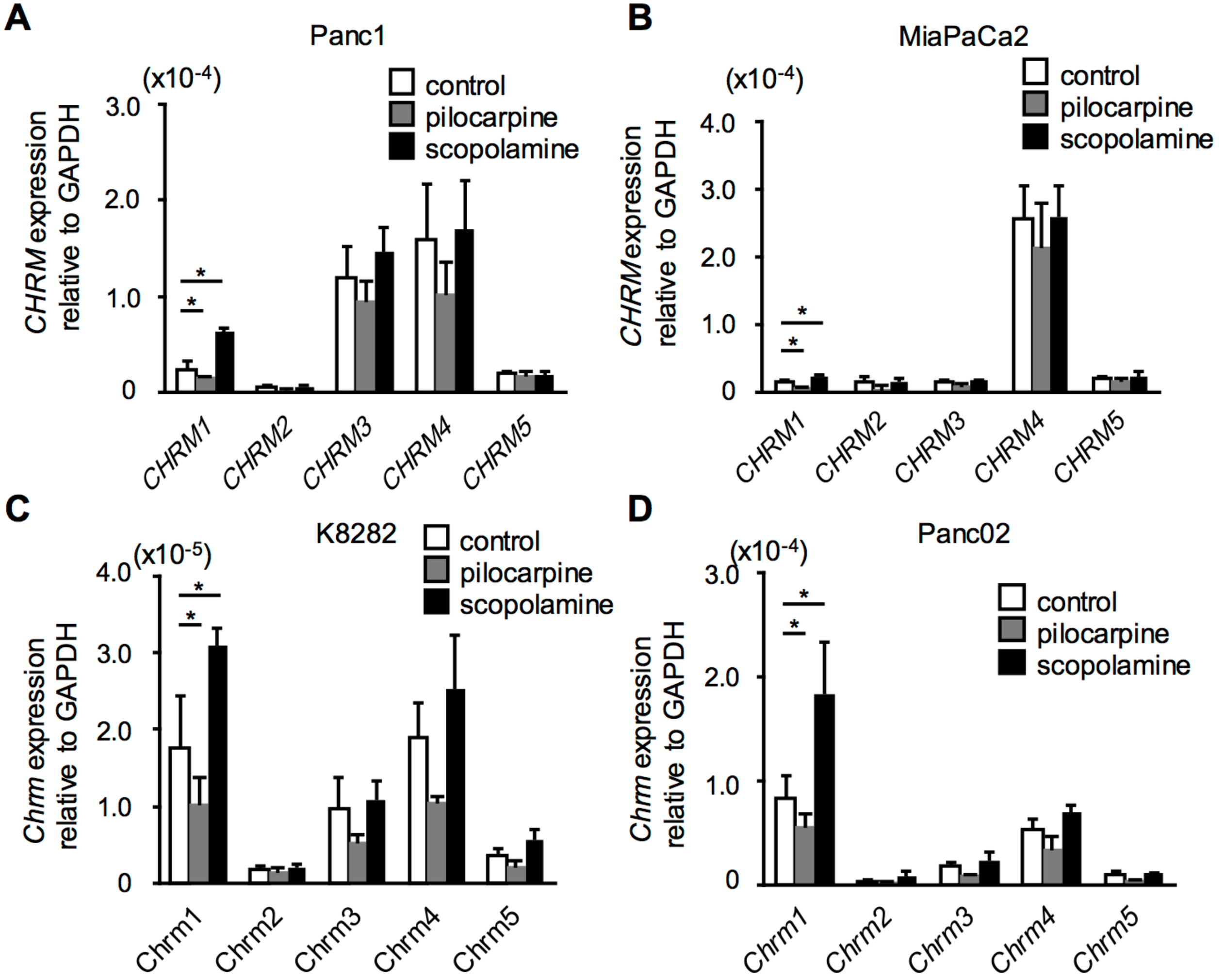

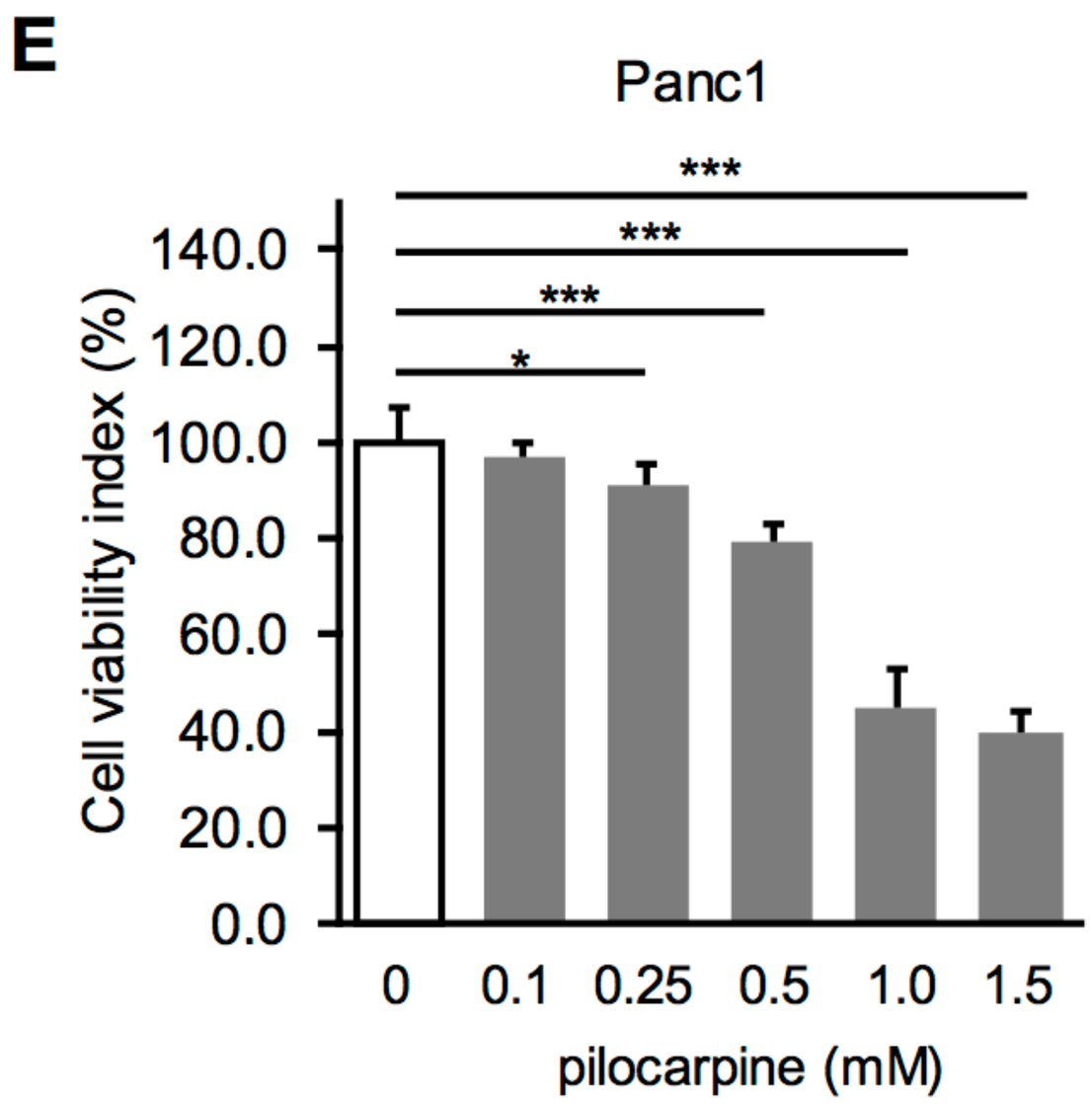

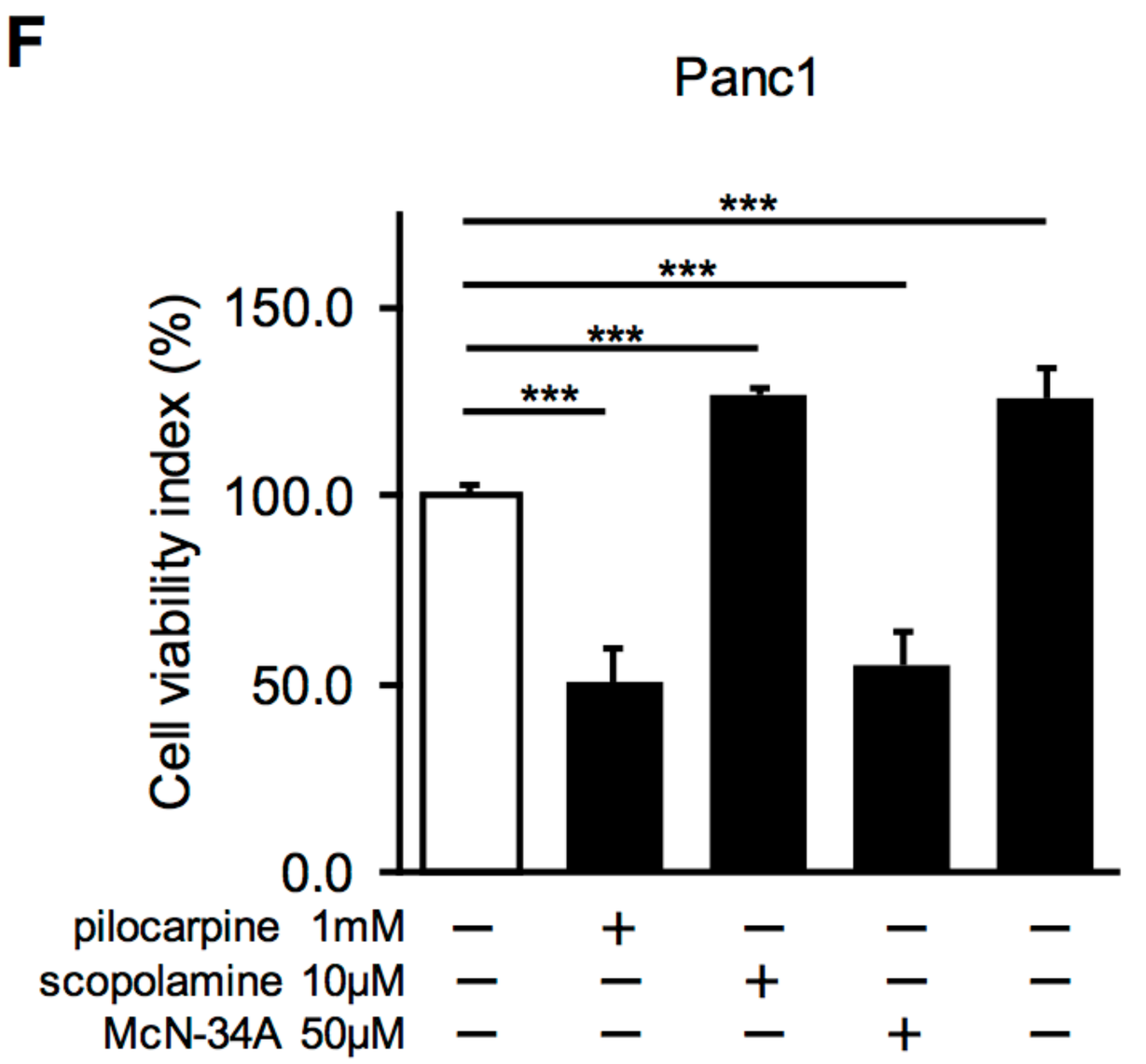

Supplementary Figure 3 (cont'd)

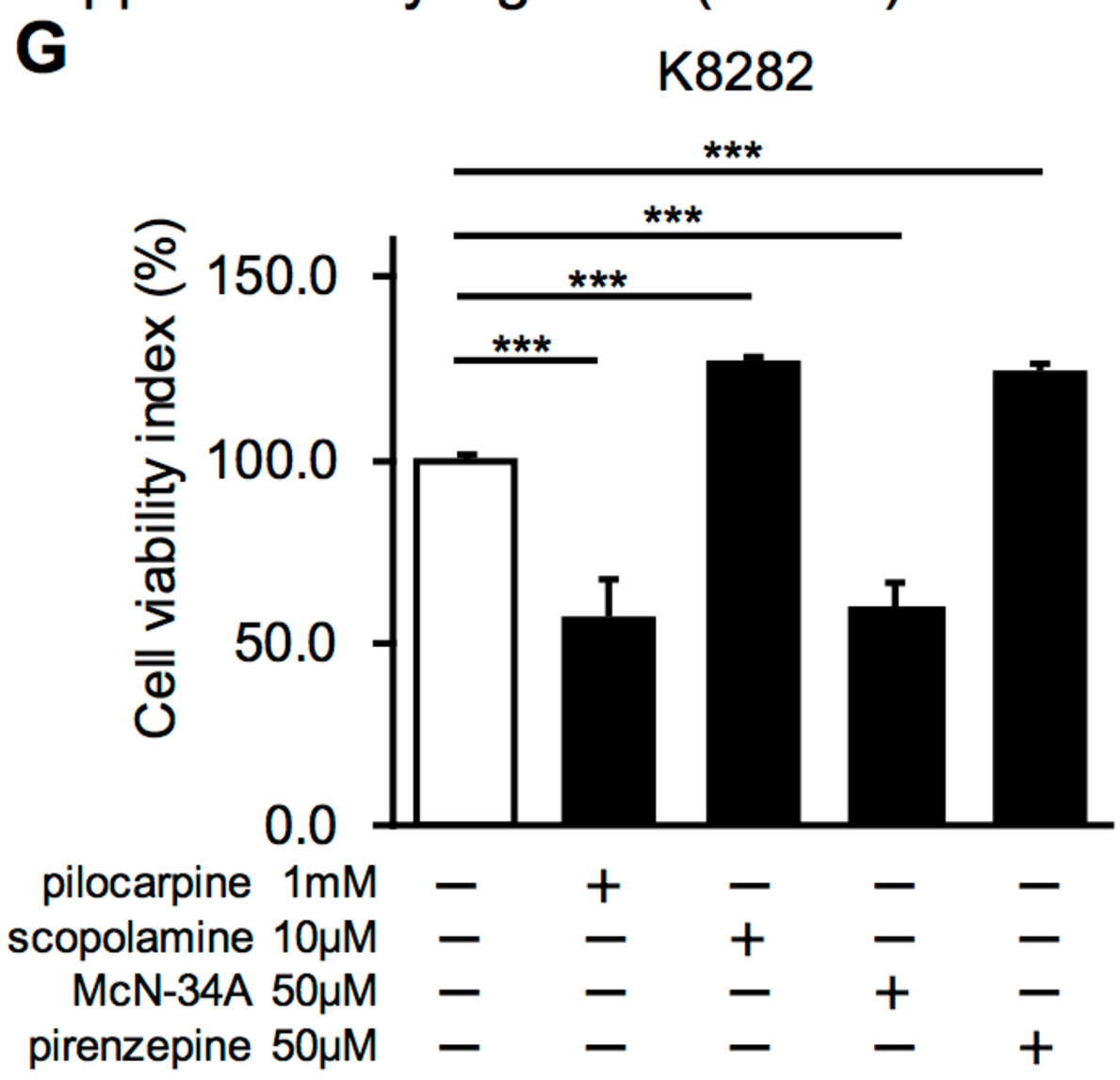

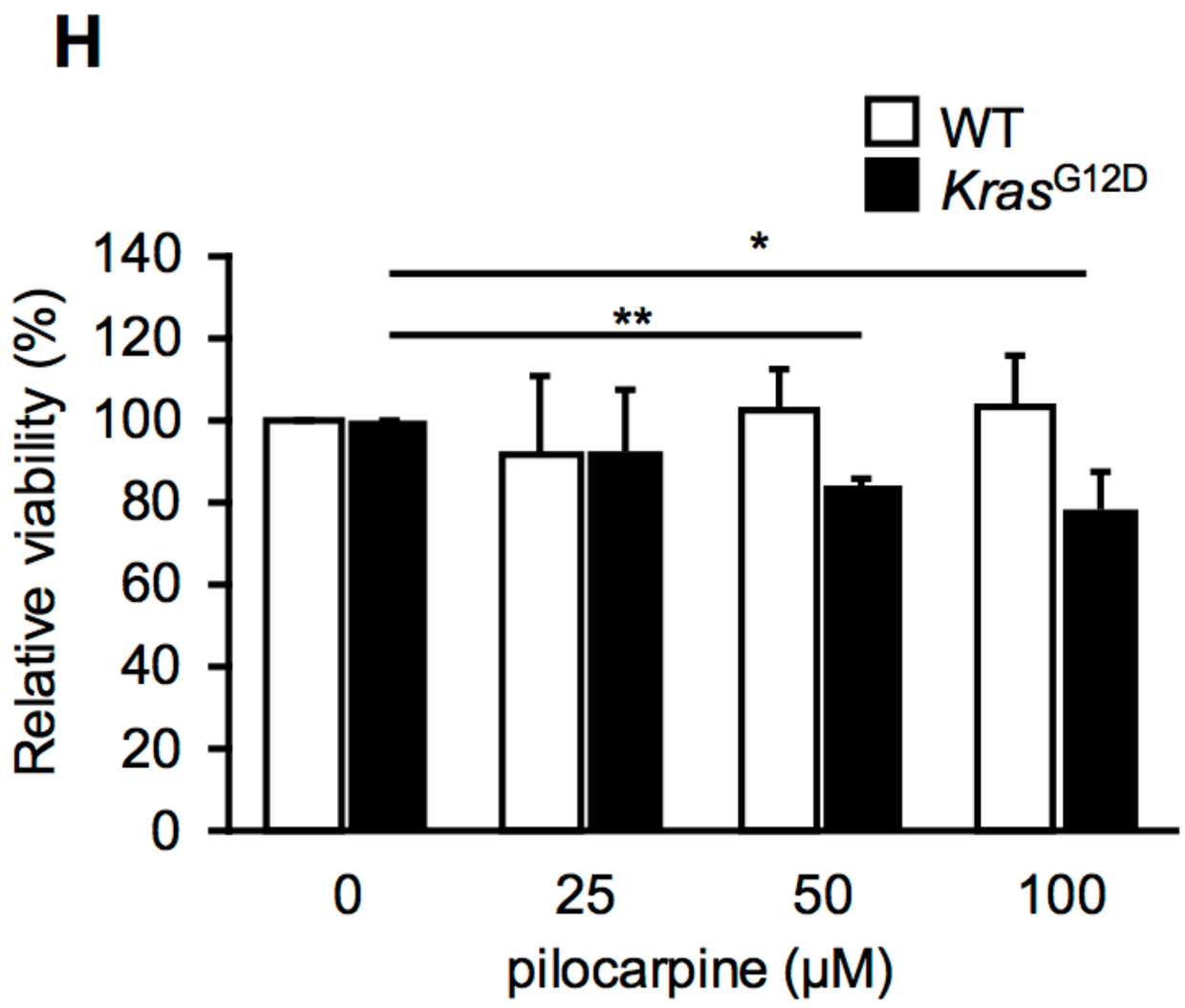

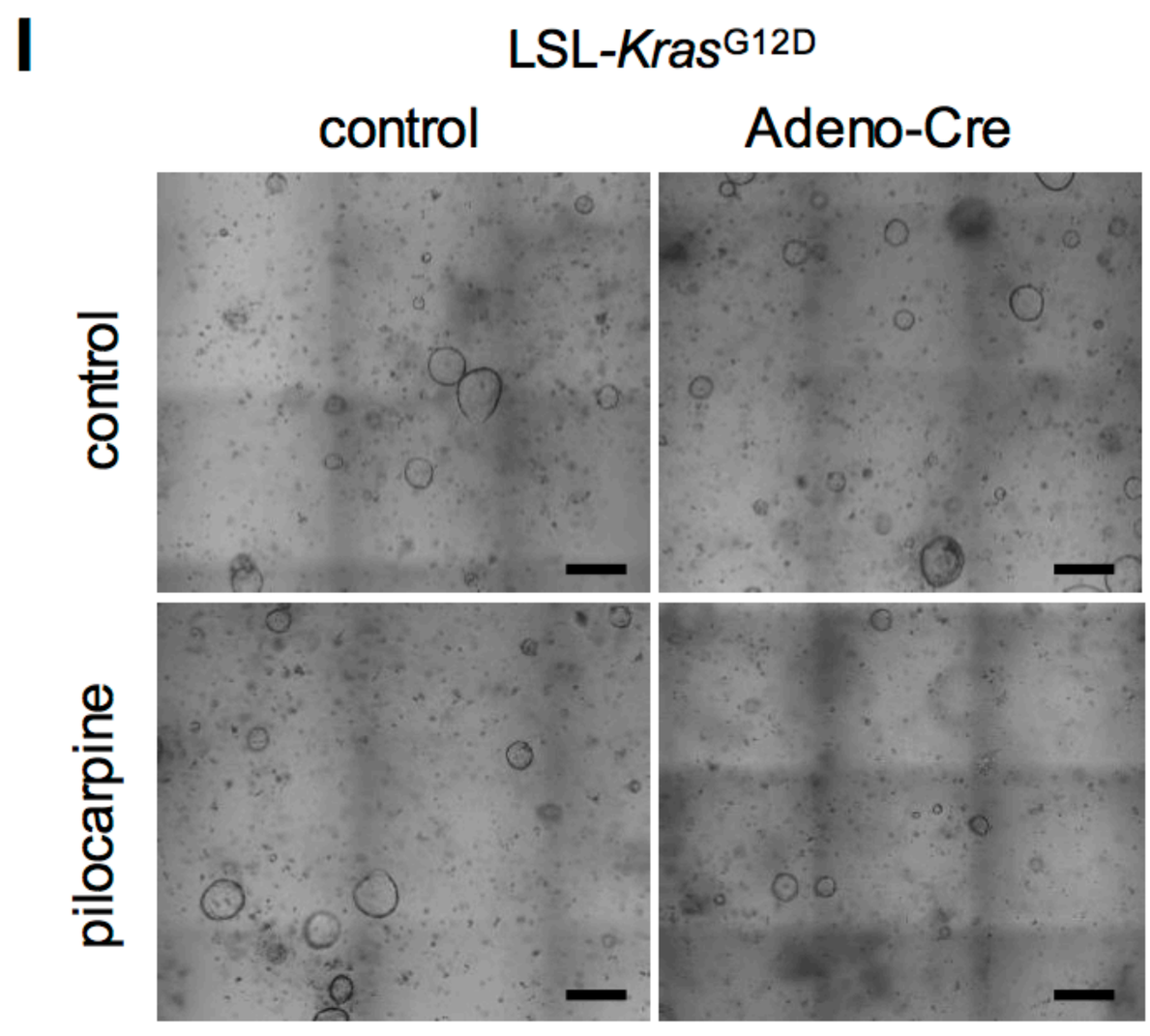

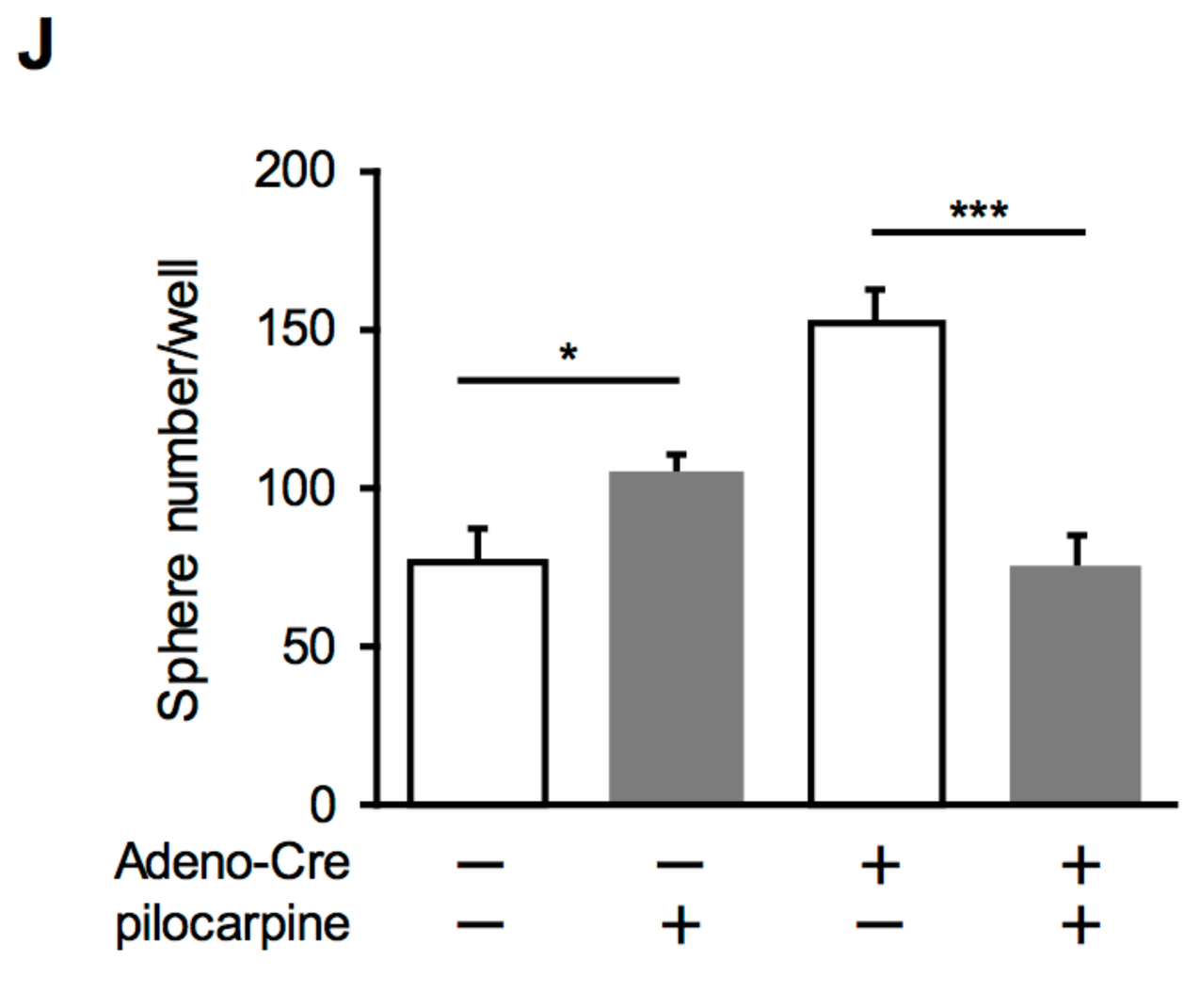

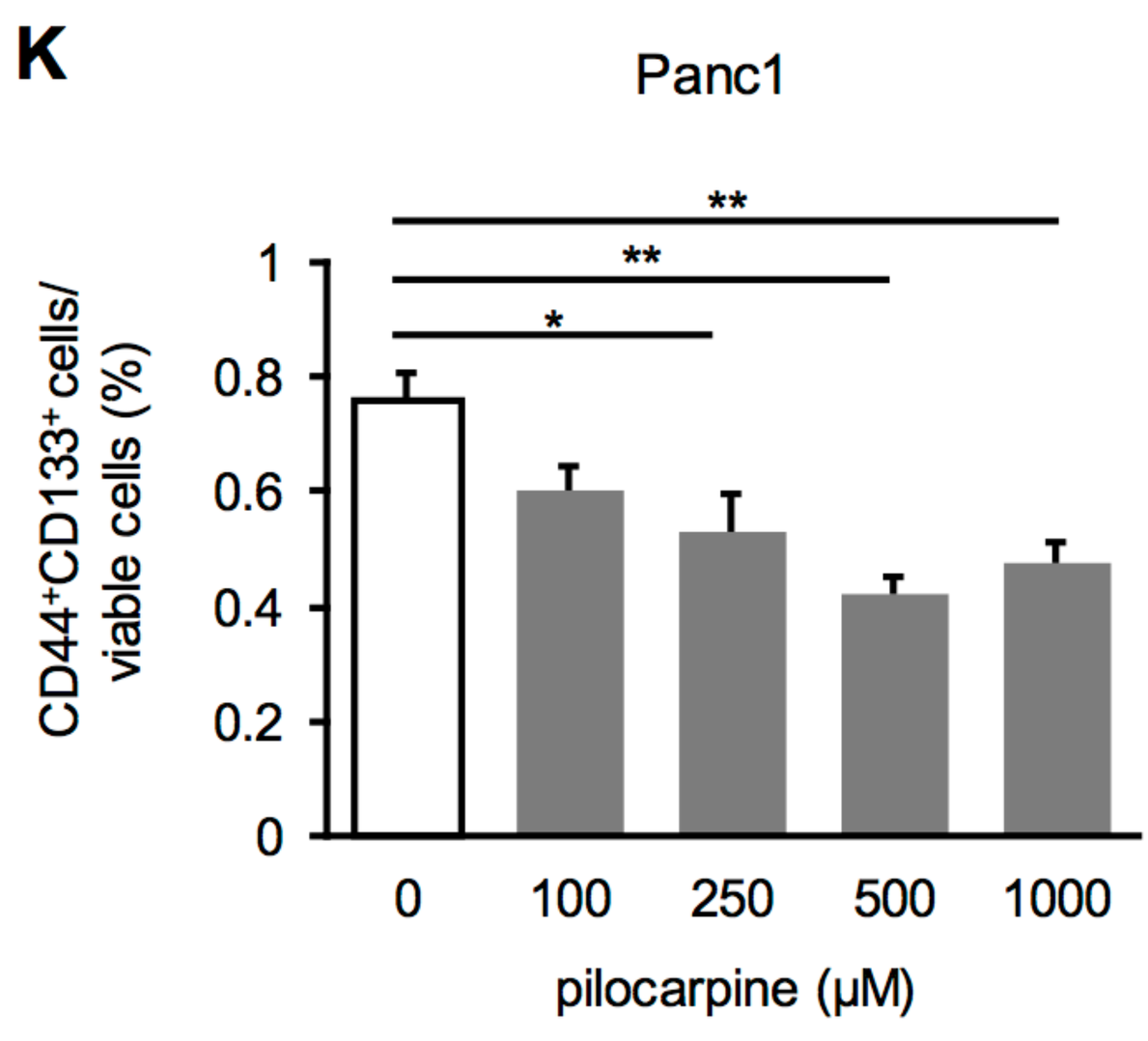

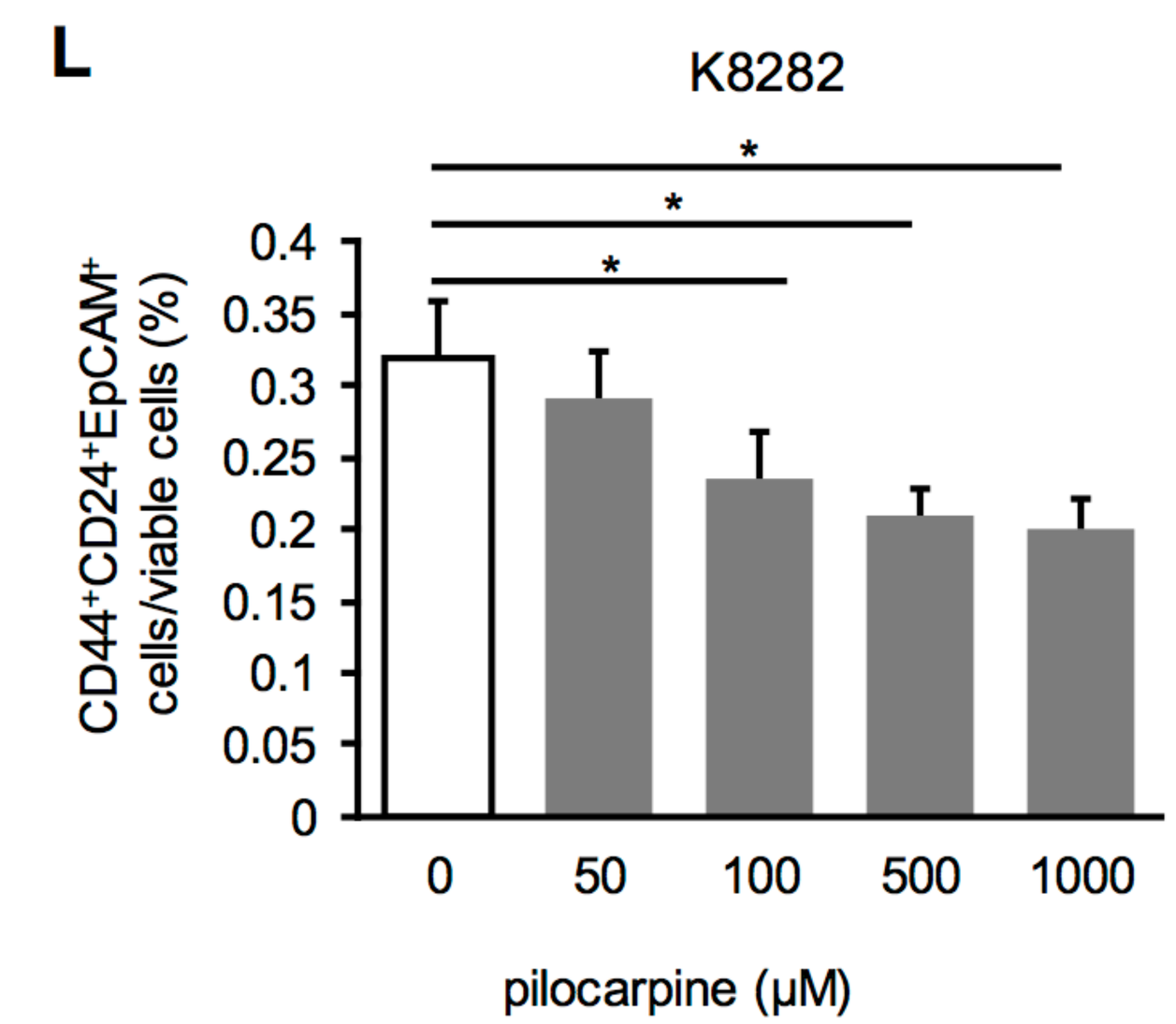

Supplementary Figure 3 (cont'd)

M

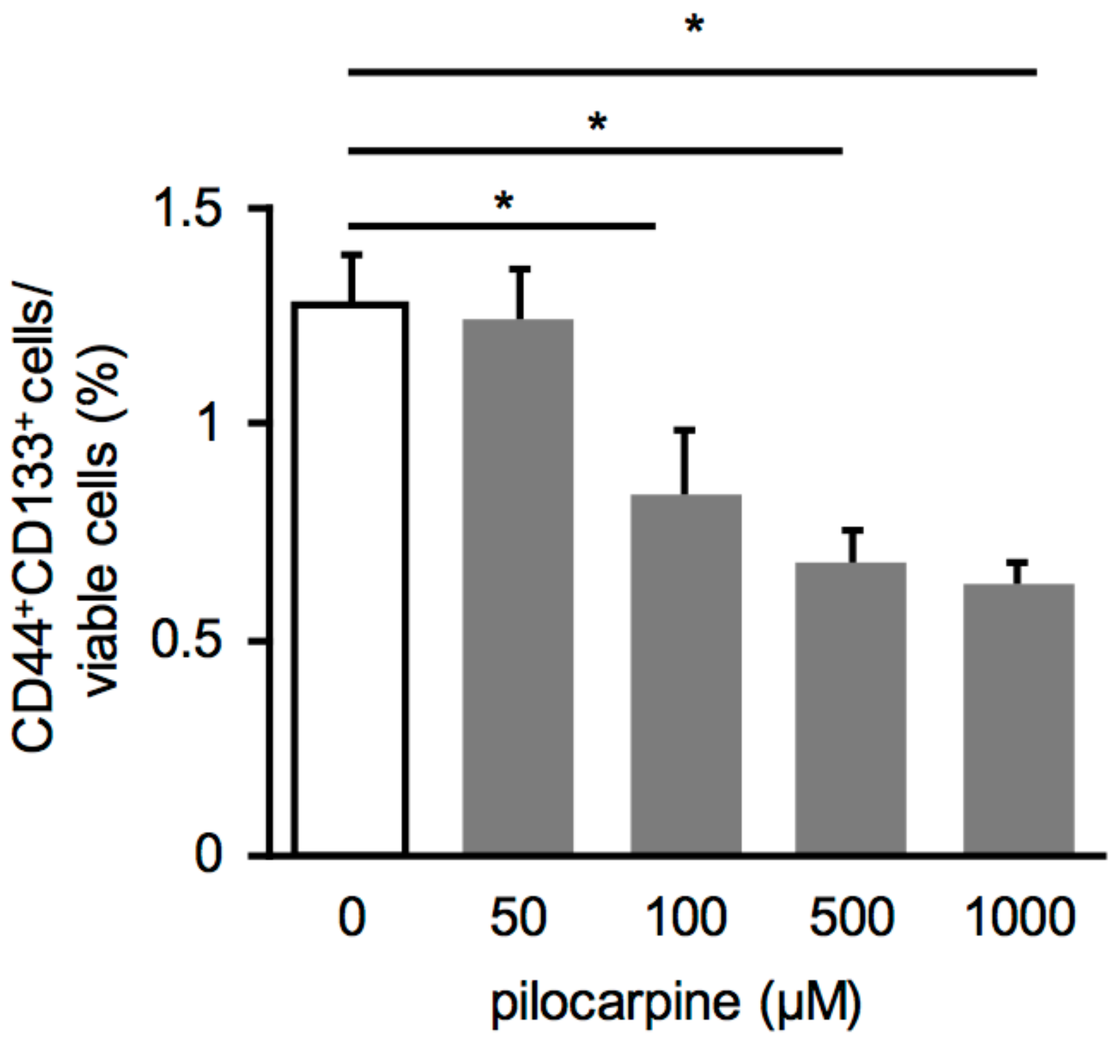

N

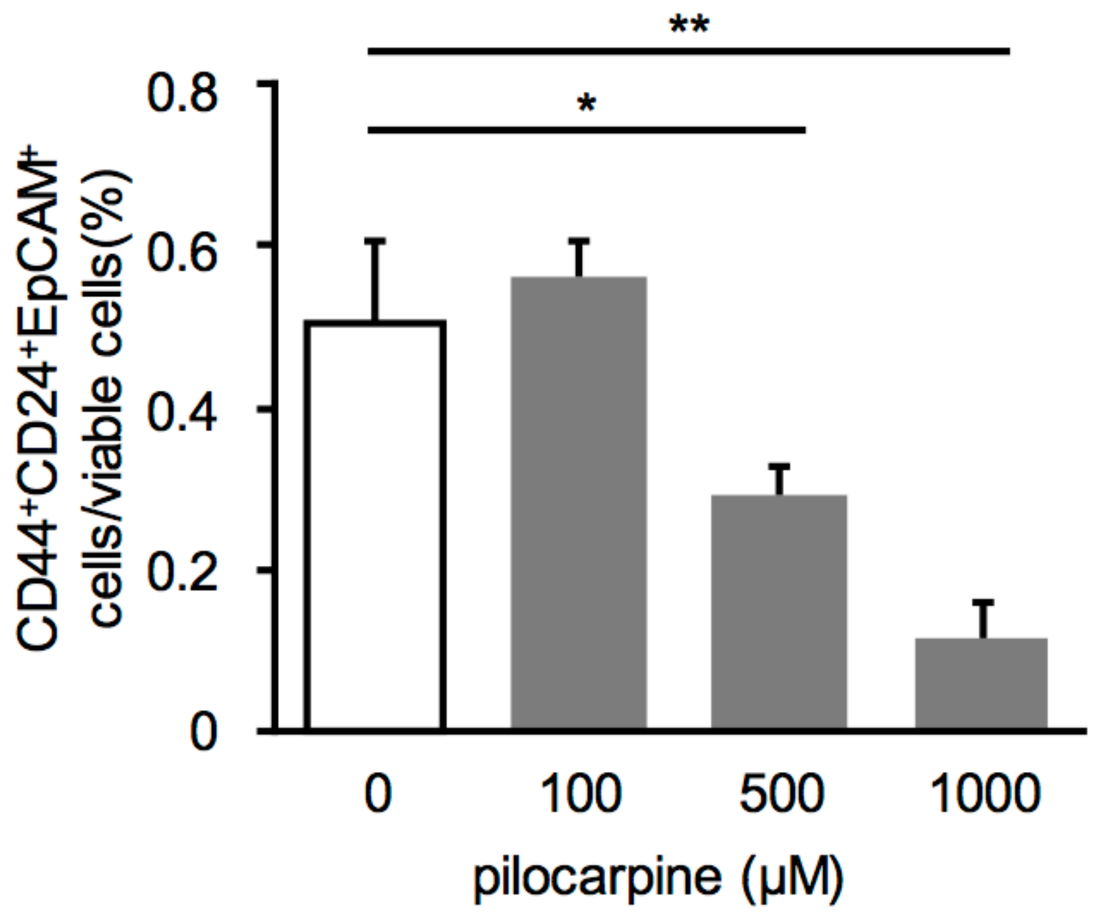

O

Q

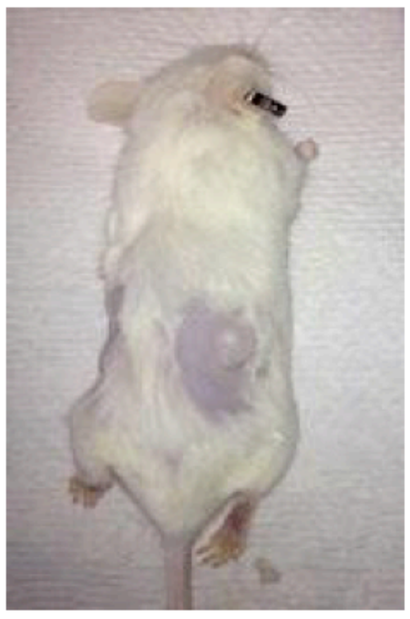

S

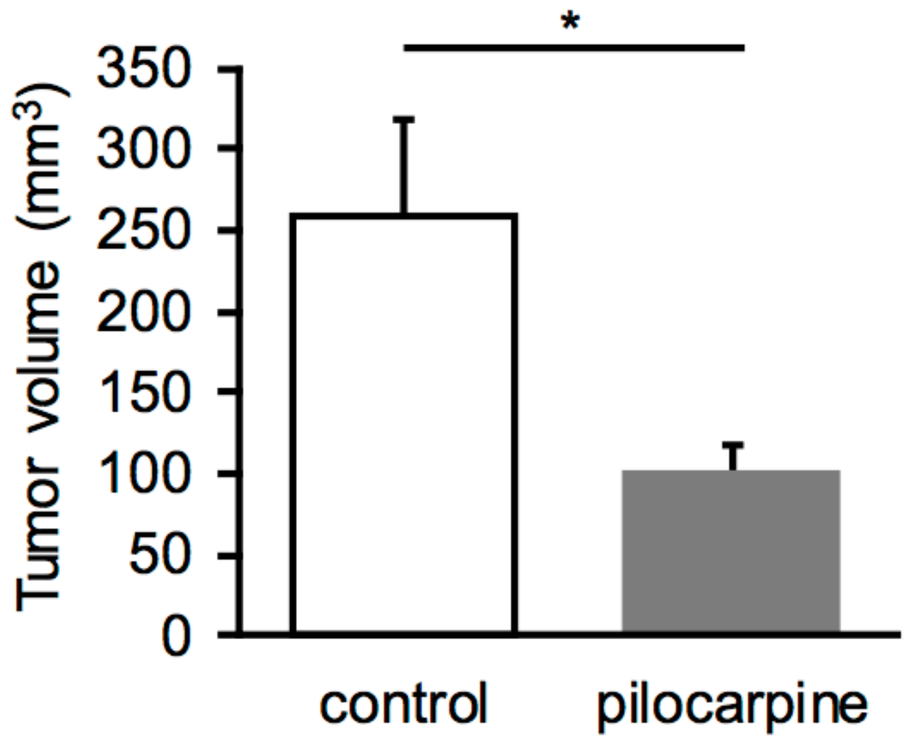

P

R

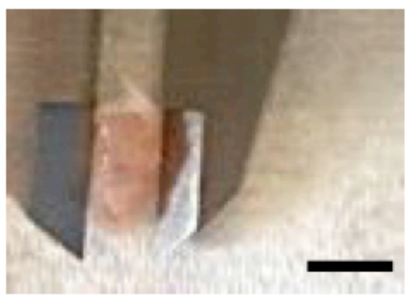

Supplementary Figure 3

A and B. Relative quantification of mRNA expression of *CHRM1-CHRM5* in human Panc1 (**A**) and MiaPaca2 (**B**) cells treated with pilocarpine or scopolamine, compared with untreated controls. **C and D.** Relative quantification of mRNA expression of *Chrm1-Chrm5* in murine K8282 (**C**) and Panc02 (**D**) cells treated with pilocarpine or scopolamine, compared with untreated controls. **E.** MTT assay of Panc1 cells treated with increasing concentrations of pilocarpine. **F.** MTT assay of Panc1 cells treated with or without pilocarpine, scopolamine, McN-A34 or pirenzepine at indicated dosages. **G.** MTT assay of K8282 cells treated with or without pilocarpine, scopolamine, McN-A34 or pirenzepine at indicated dosages. **H.** MTT assay of WT HPDE-E6E7 (WT) or *Kras*^{G12D} HPDE-E6E7 *(Kras*^{G12D}*)* cells treated with increasing concentrations of pilocarpine. **I.** Representative images of pancreatic spheres isolated from LSL-*Kras*$^{+/G12D}$ mice and treated with or without an Adeno-Cre virus and with or without pilocarpine; Scale bars, 500 μm. **J.** Bar graph showing quantification of number of pancreatic spheres per well isolated from LSL-*Kras*$^{+/G12D}$ mice, treated with or without an Adeno-Cre virus and with or without pilocarpine. **K.** Bar graph showing quantification of flow cytometric analysis of $CD44^+CD133^+$ cells in Panc1 cells treated with increasing concentrations of pilocarpine. **L.** Bar graph showing quantification of flow cytometric analysis of $CD44^+CD24^+EpCAM^+$ cells in K8282 cells treated with increasing concentrations of pilocarpine. **M.** Bar graph showing quantification of flow cytometric analysis of $CD44^+CD133^+$ cells in K8282 cells treated with increasing concentrations of pilocarpine. **N.** Bar graph showing quantification of flow cytometric analysis of $CD44^+CD24^+EpCAM^+$ cells in K2548 cells treated with increasing concentrations of pilocarpine. **O and P.** Representative gross images of subcutaneous tumors in NOD/SCID mice 6 weeks after implantation of 25,000 Panc1 cells (**O**) and resected tumor (**P**). **Q and R.** Representative gross images of subcutaneous tumors in NOD/SCID mice 6 weeks after implantation of 25,000 Panc1 cells pretreated for 72 hours with pilocarpine (**Q**) and resected tumor (**R**). **S.** Volume of tumors in NOD/SCID mice 6 weeks after injection of 25,000 implanted Panc1 cells with and without pretreatment of pilocarpine. Scale bars, 5 mm. Mean s± SD in Fig. A-G and Means ± SEM in Fig. H, J-N and S. *$p < 0.05$; **$p < 0.01$; ***$p < 0.001$.

Supplementary Figure 4

A

	SYMBOL	ENTREZID	log_2FC	FC(Ratio)	P.Value	fdr
1	KDR(RTK)	3791	-1.31	0.40	1.0E-04	6.2E-04
2	NTRK2(TRKB)	4915	-1.18	0.44	3.39E-05	3.32E-04
3	EGFR	1956	-1.06	0.48	5.2E-05	4.1E-04
4	ITGAV(ITGA)	3685	-0.73	0.60	4.2E-05	3.7E-04
5	BRAF(RafB)	673	-0.65	0.64	6.6E-04	2.3E-03
6	PIK3CA(PI3K)	5290	-0.63	0.64	8.4E-05	5.4E-04

B

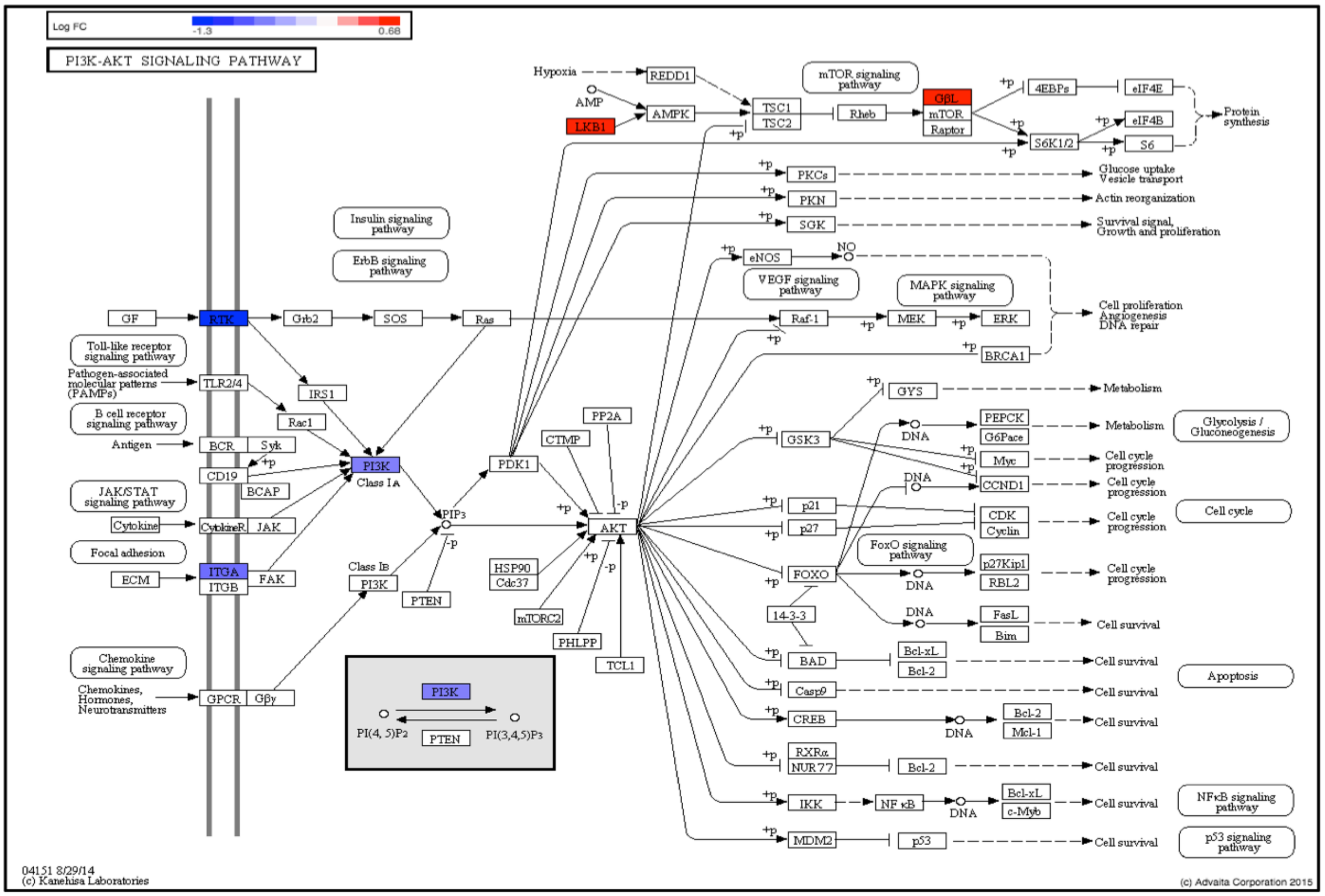

C

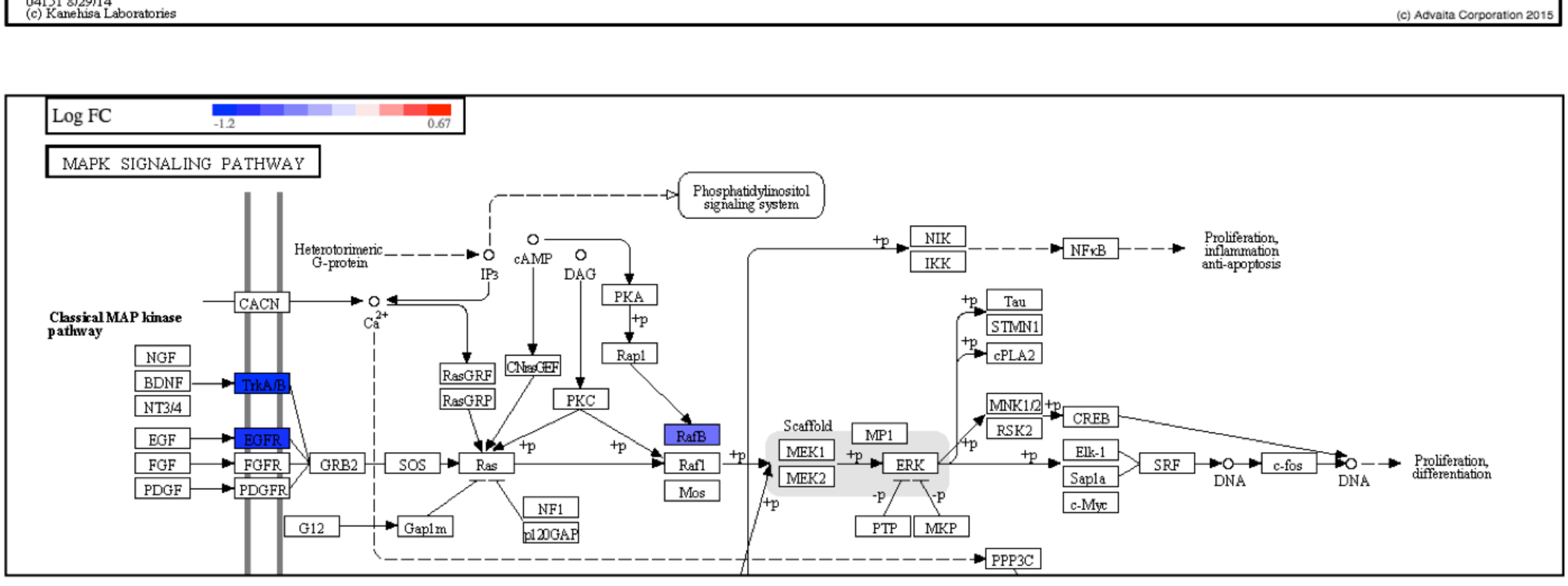

Supplementary Figure 4 (cont'd)

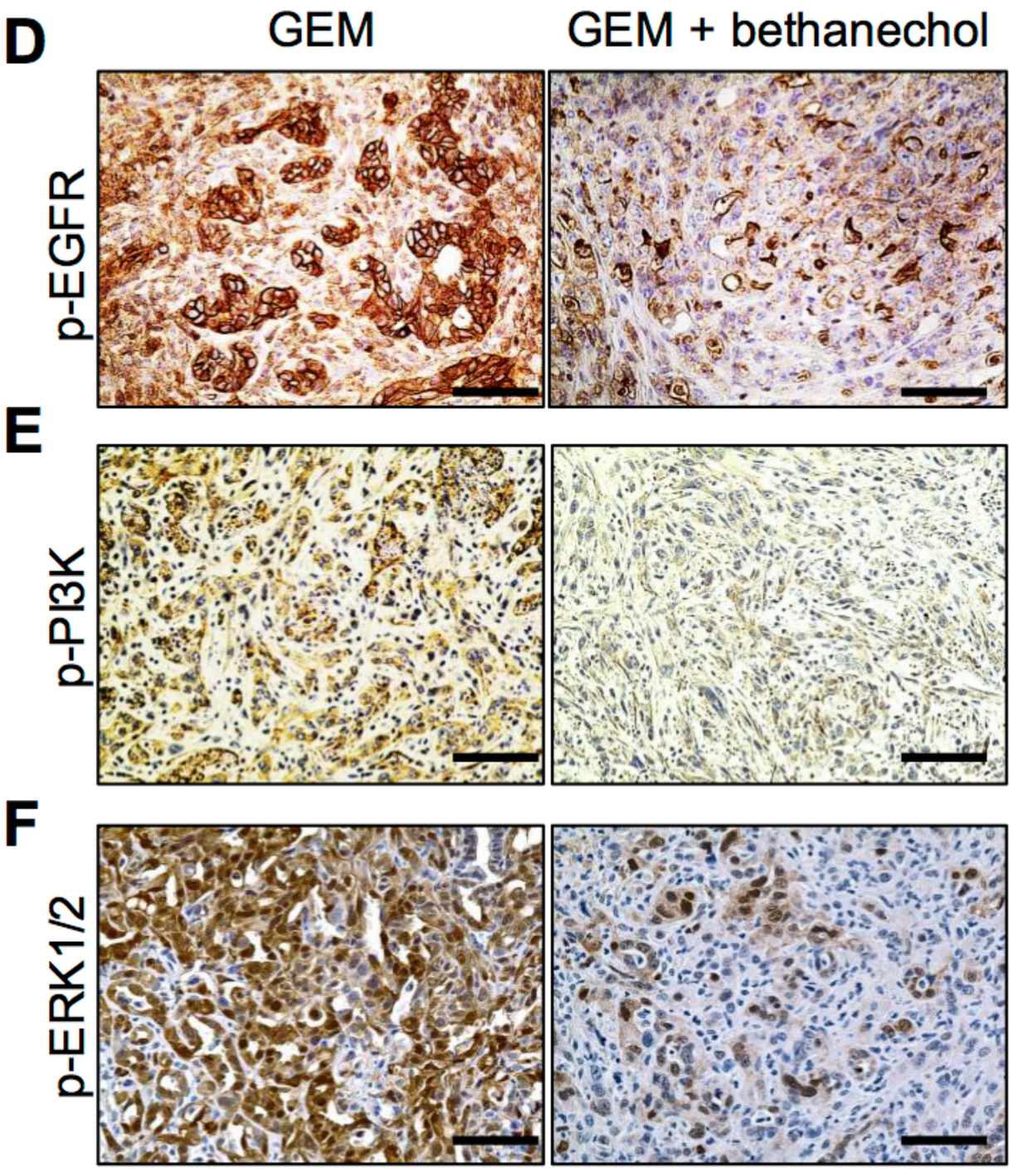

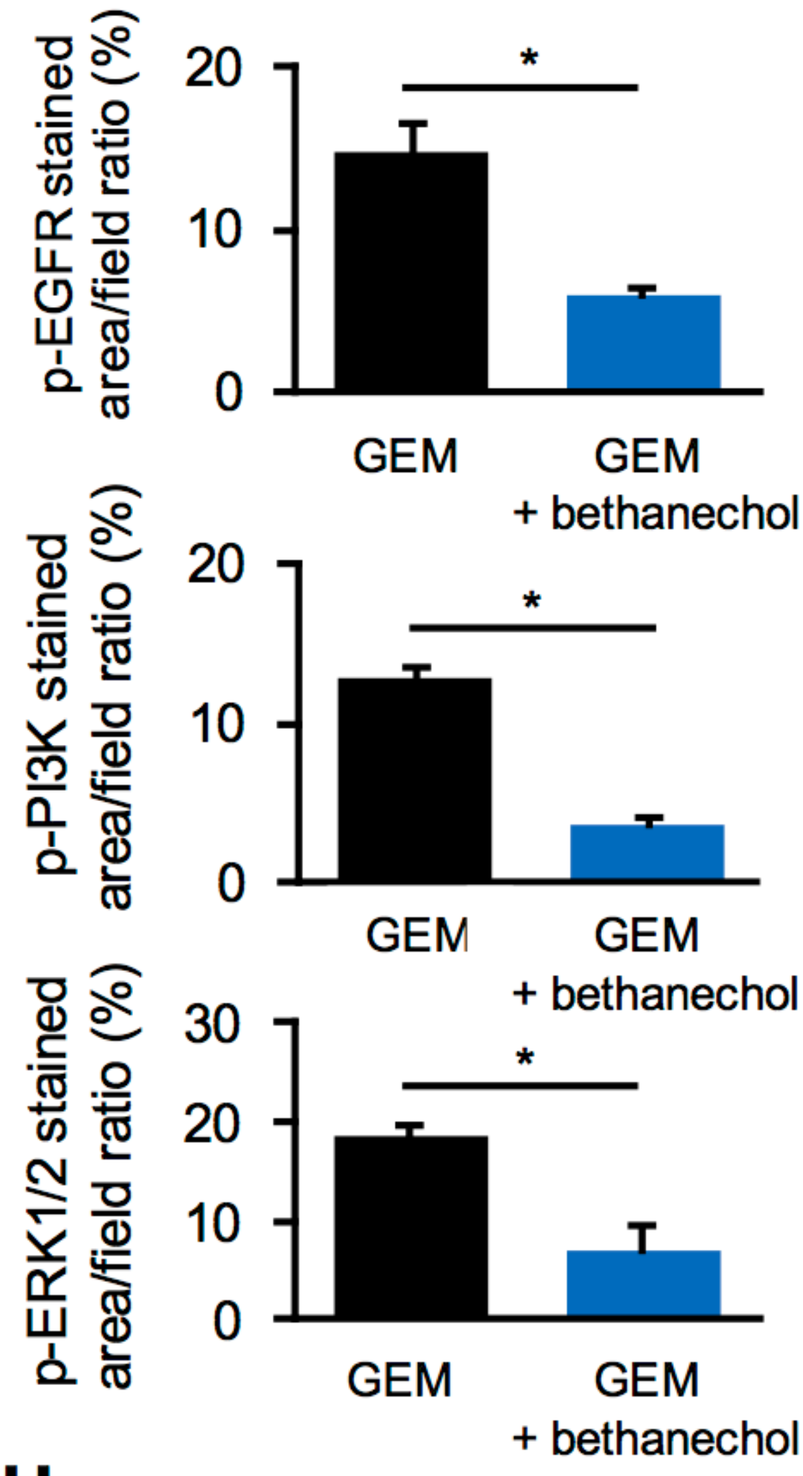

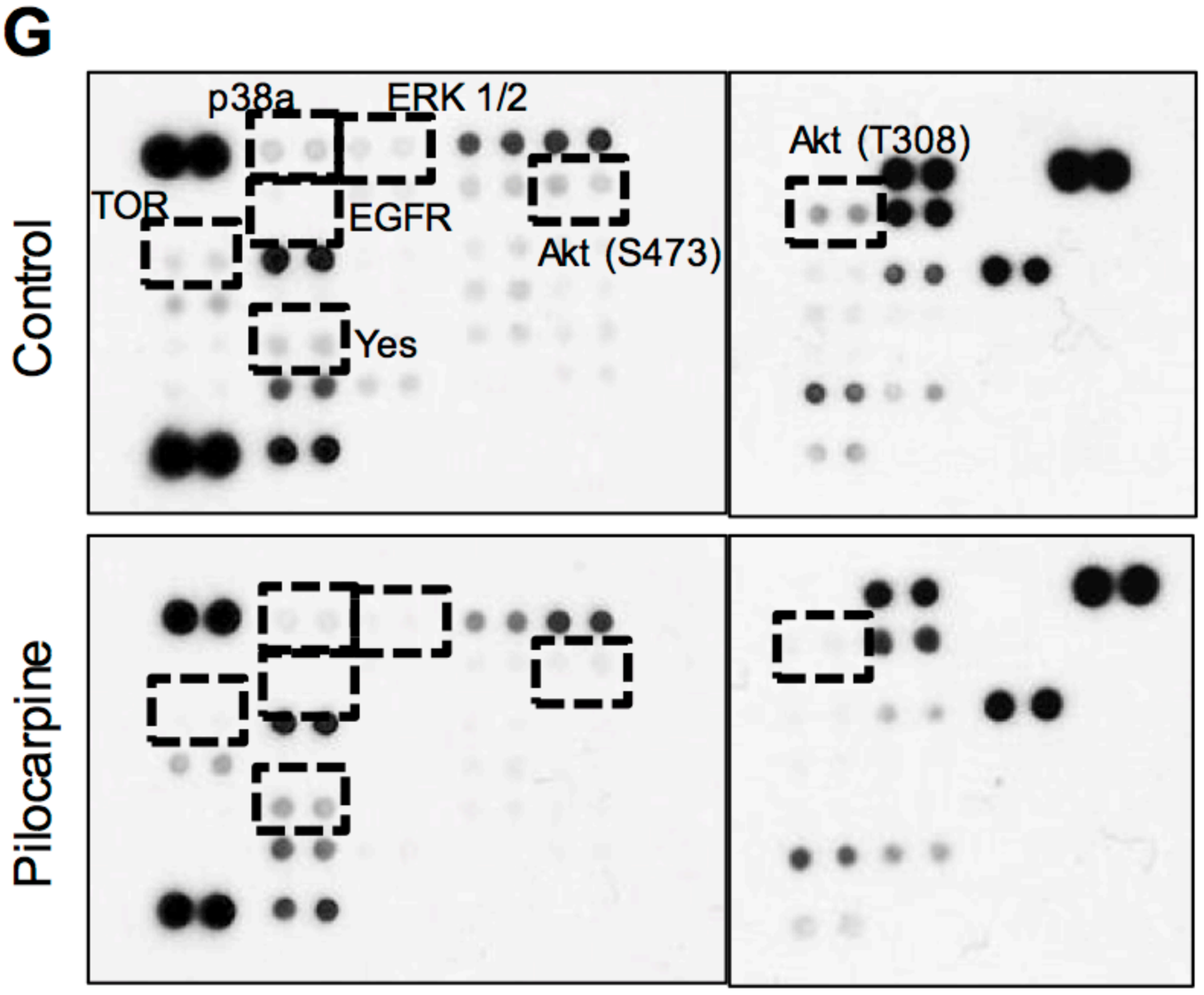

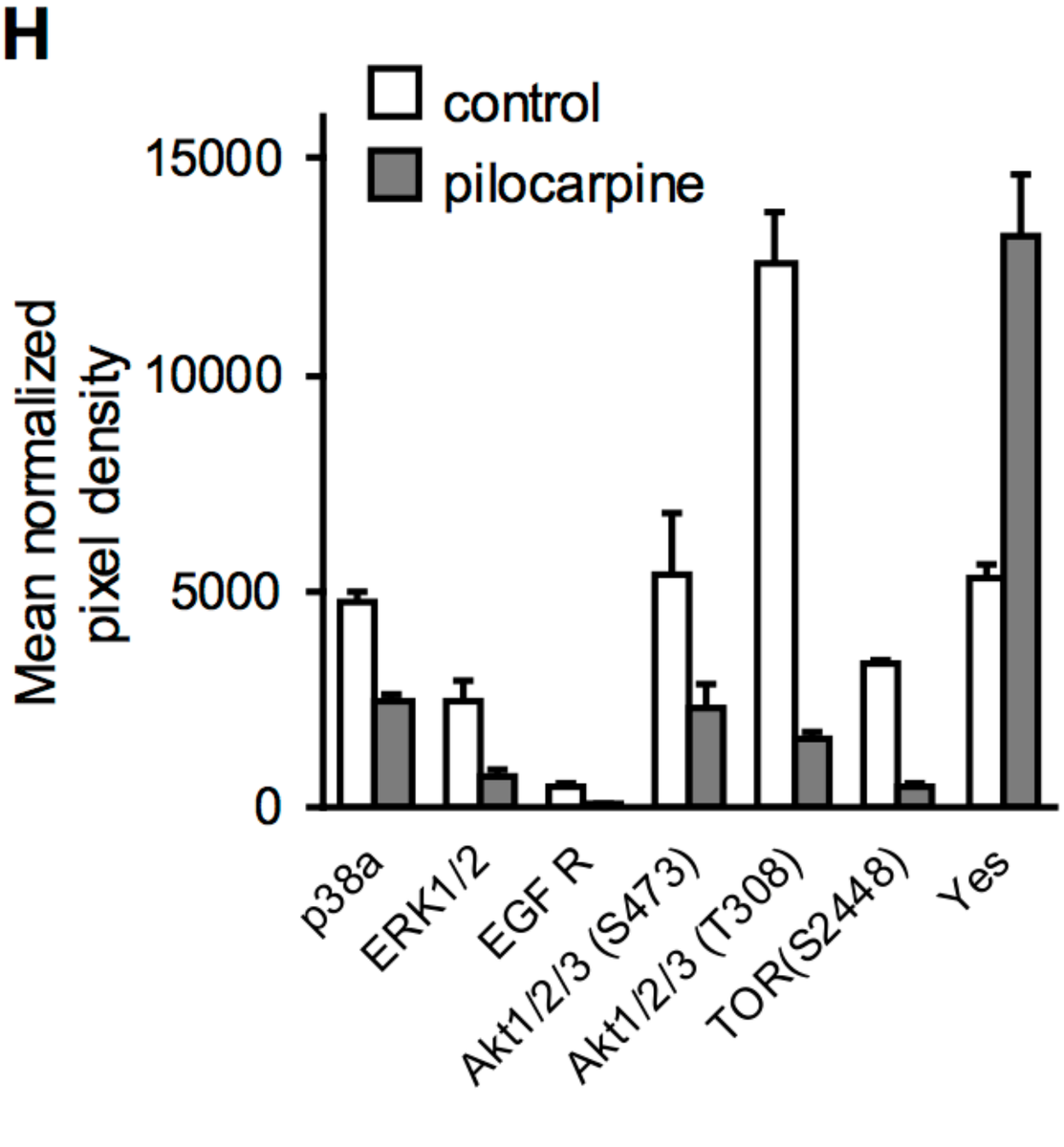

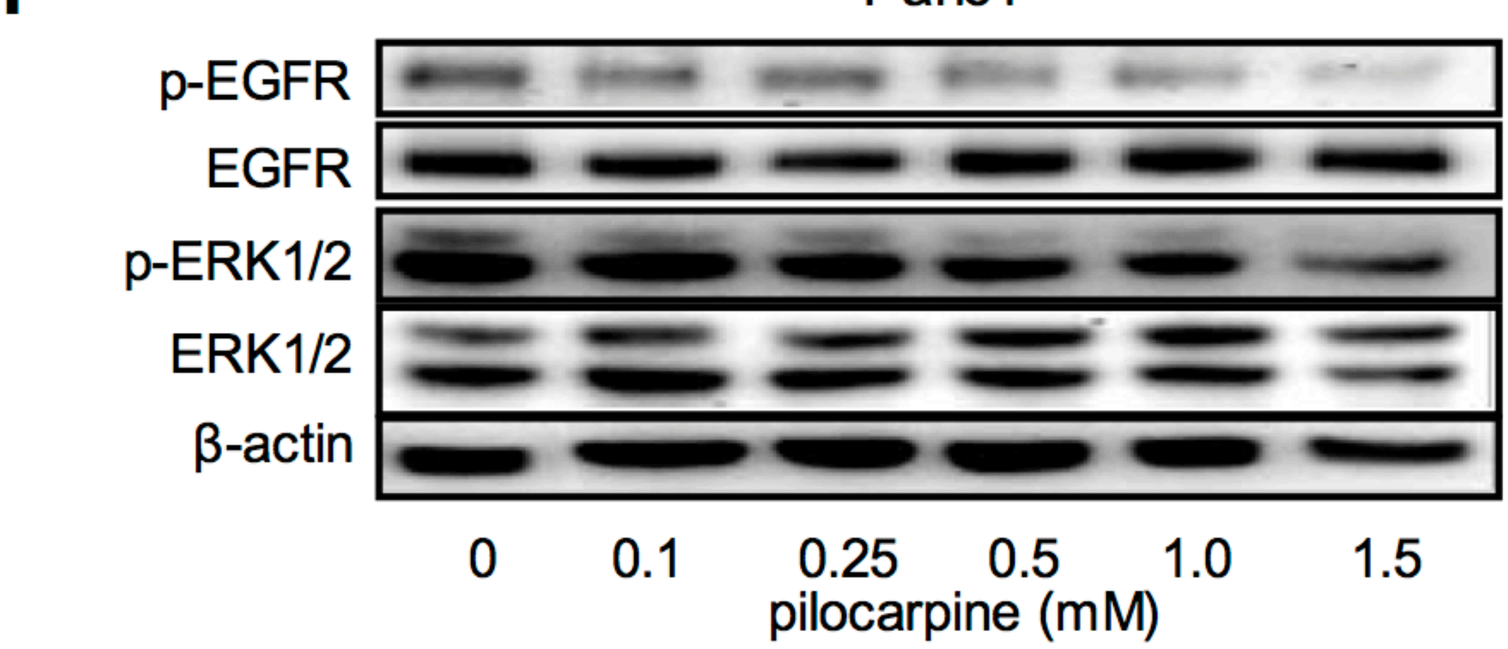

Supplementary Figure 4 (cont'd)

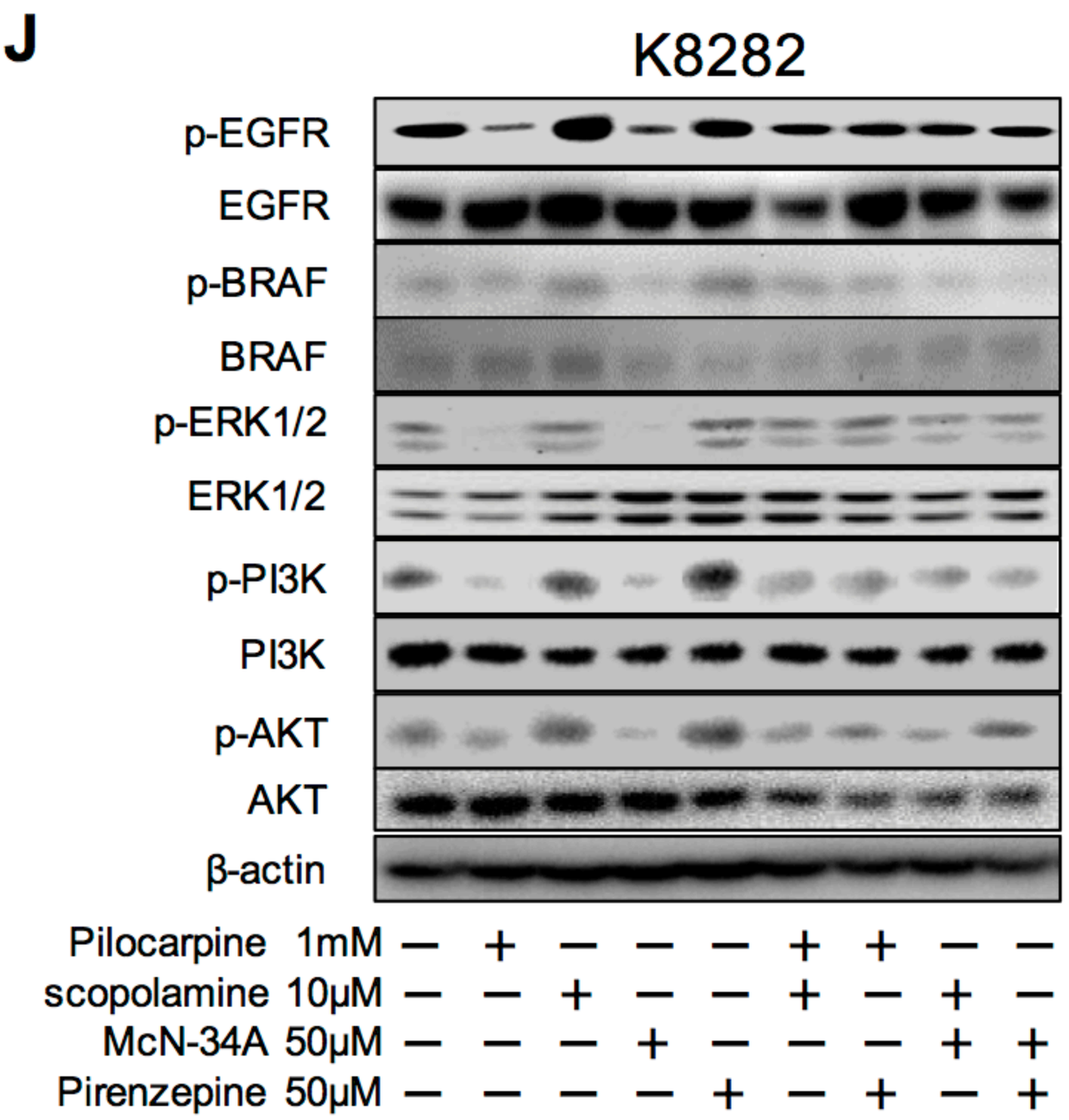

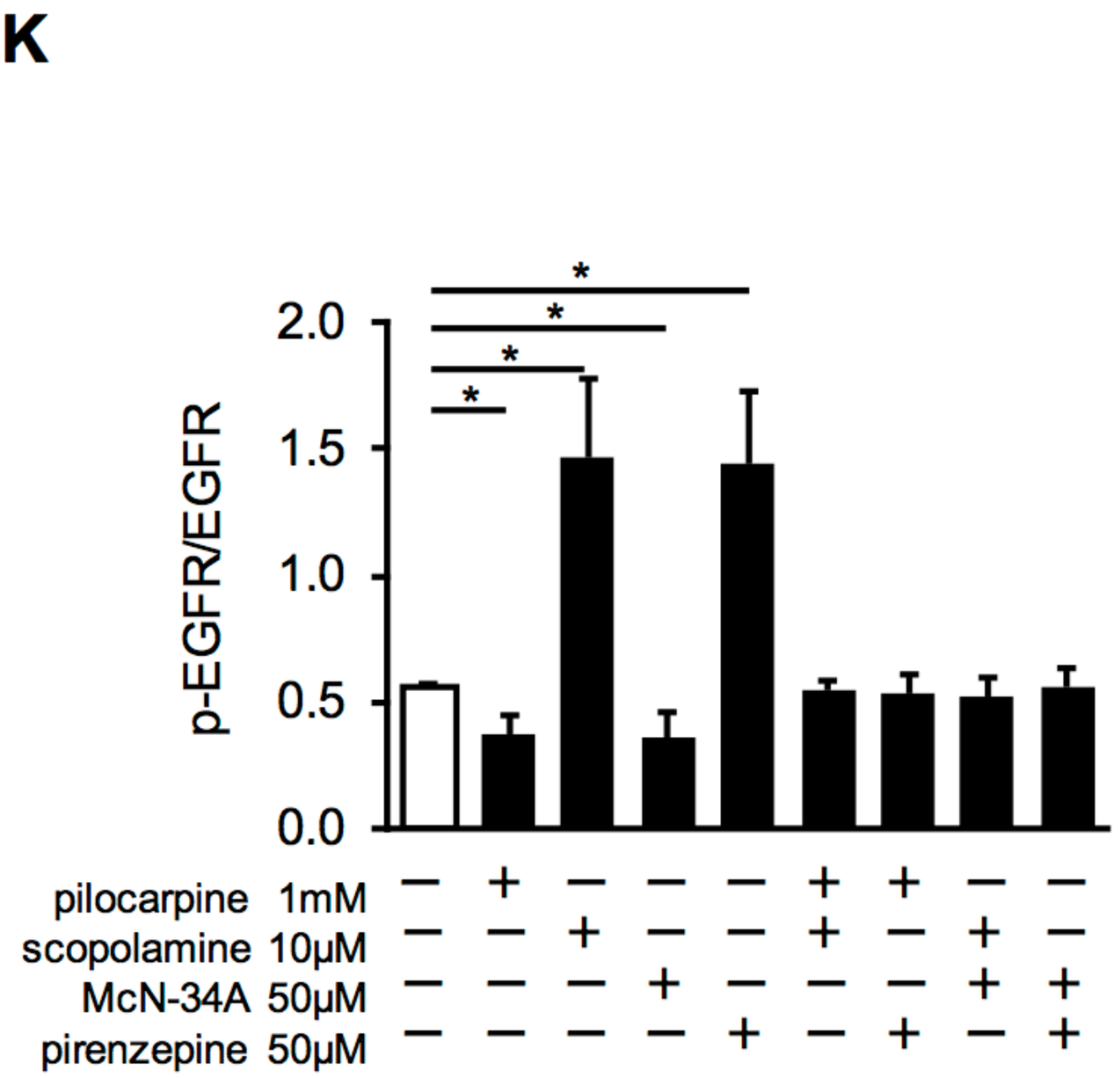

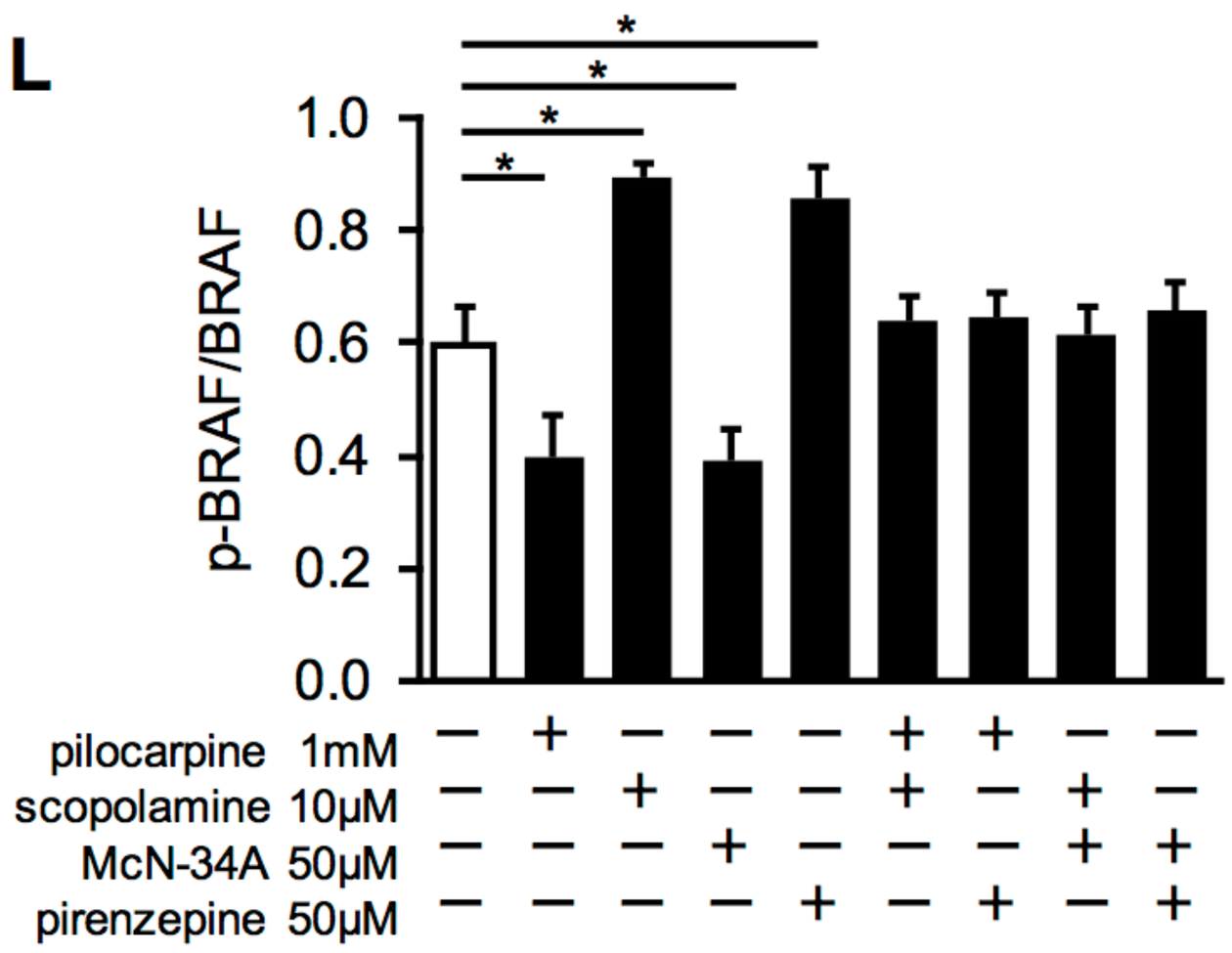

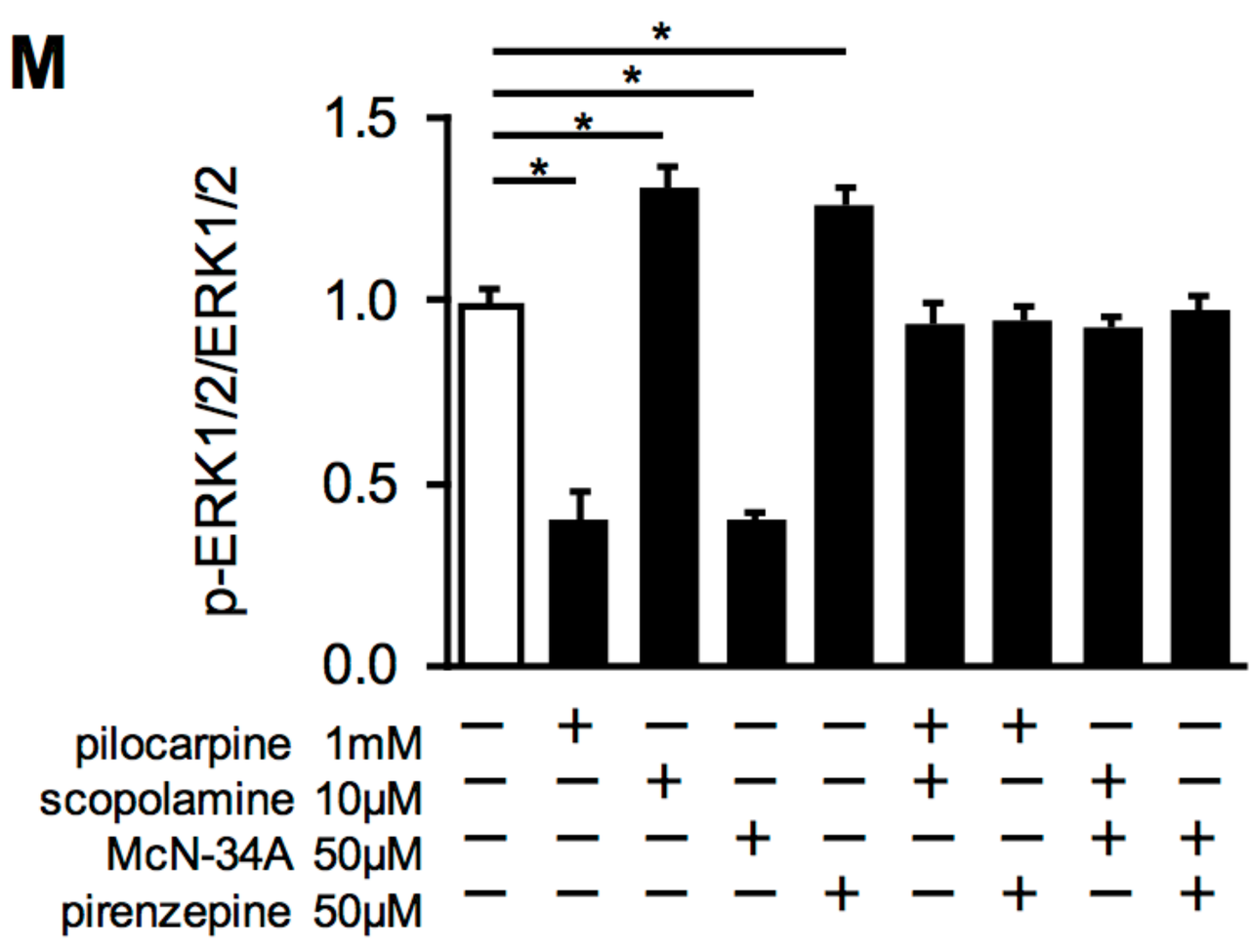

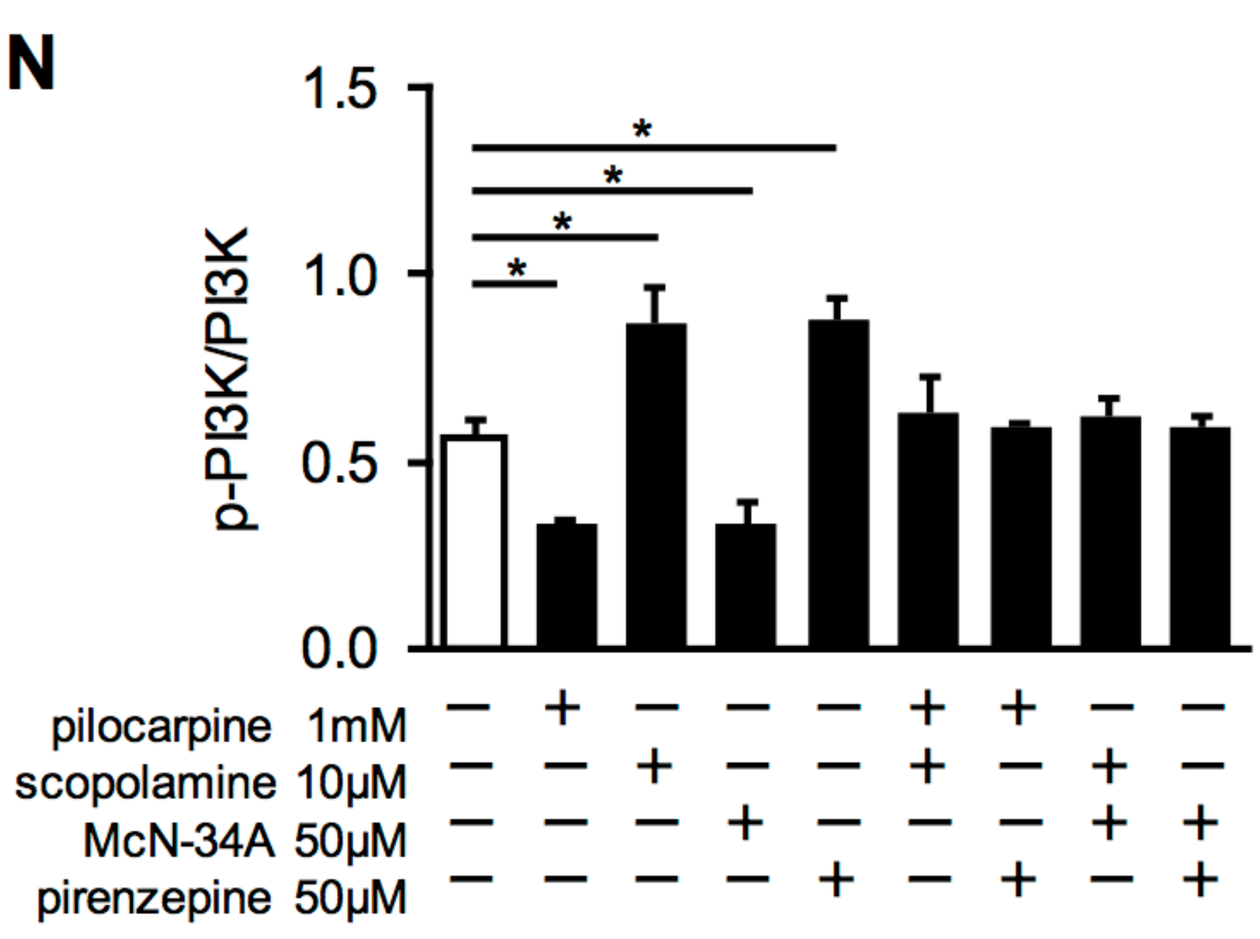

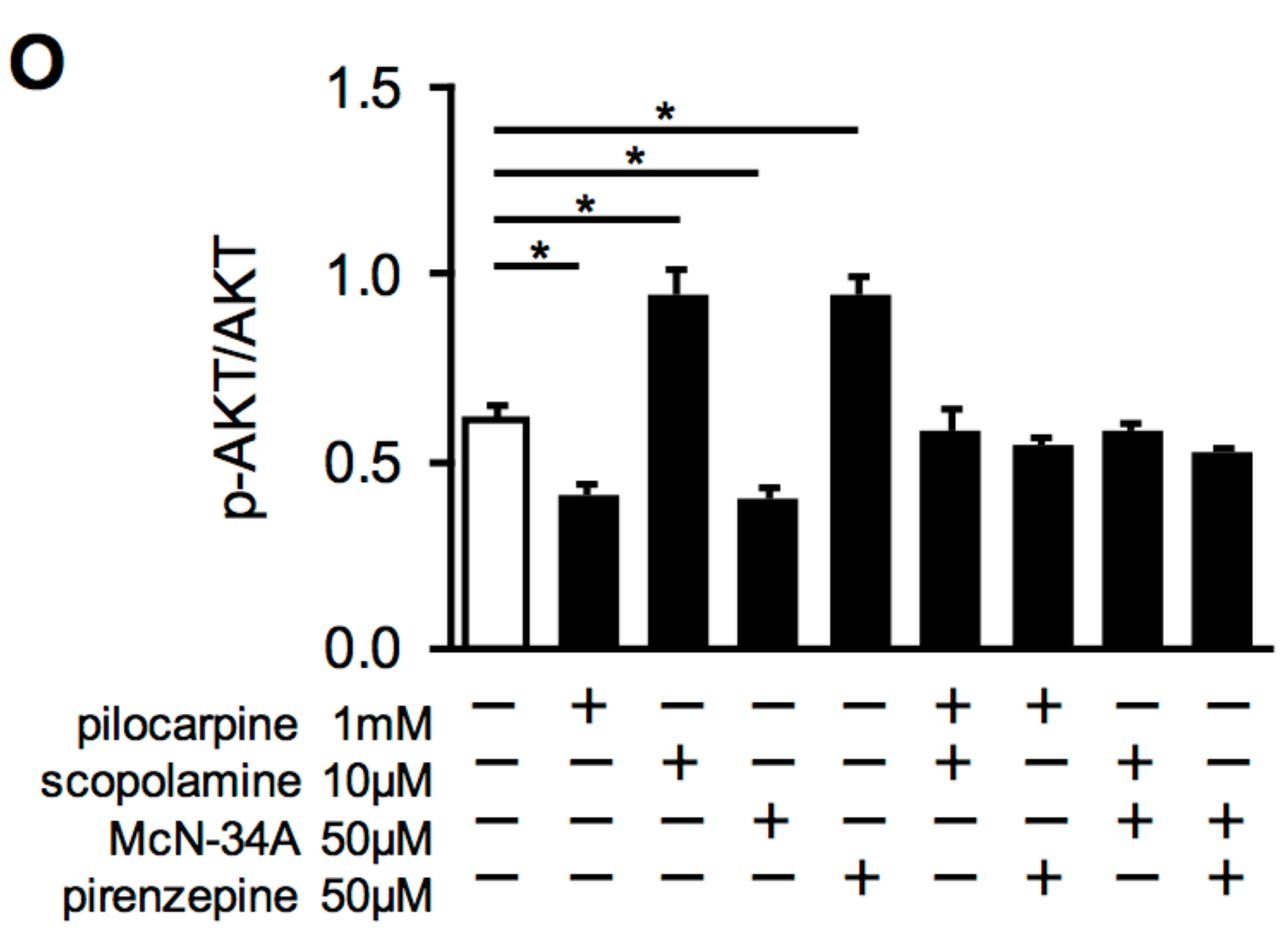

Supplementary Figure 4 (cont'd)

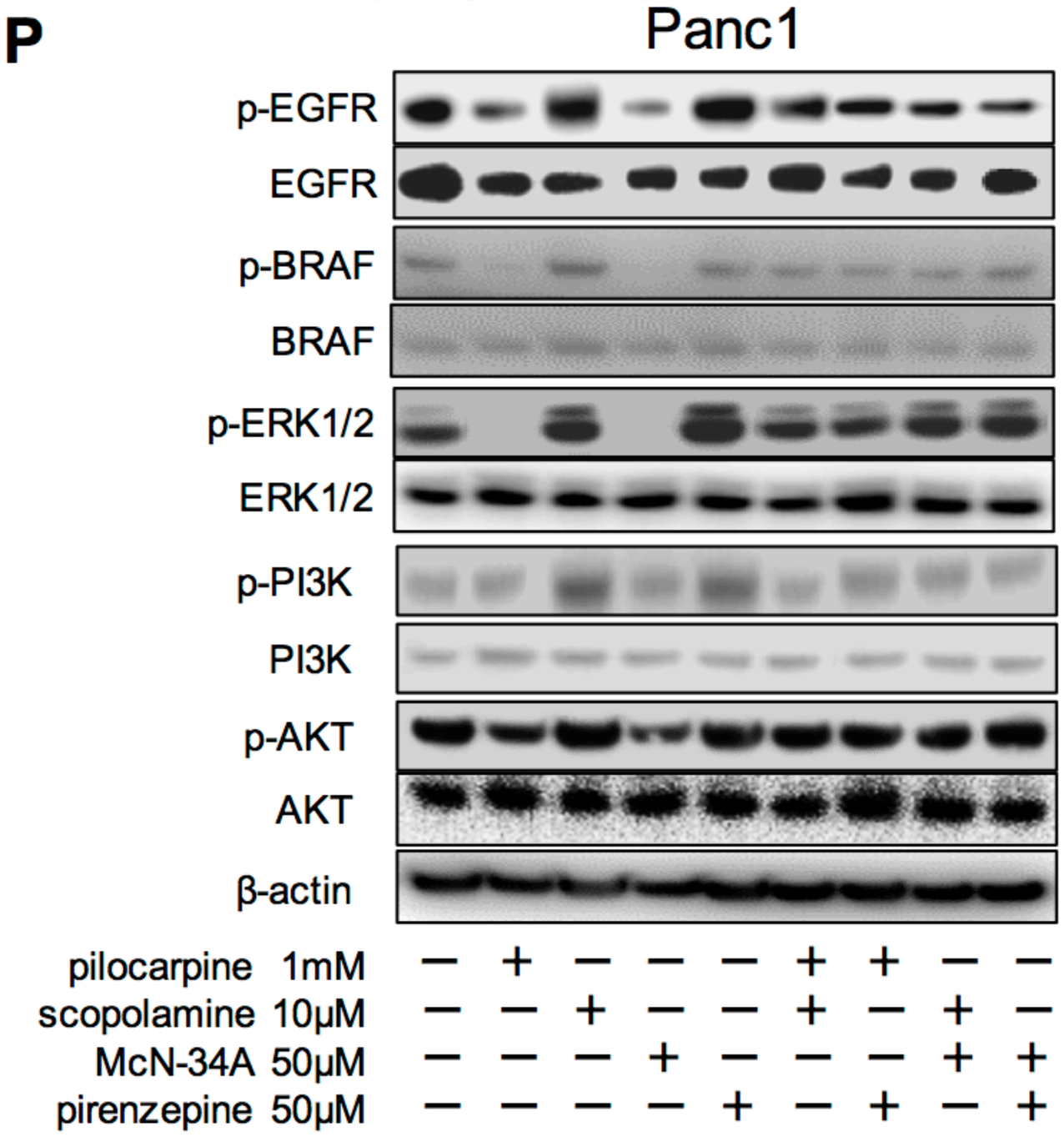

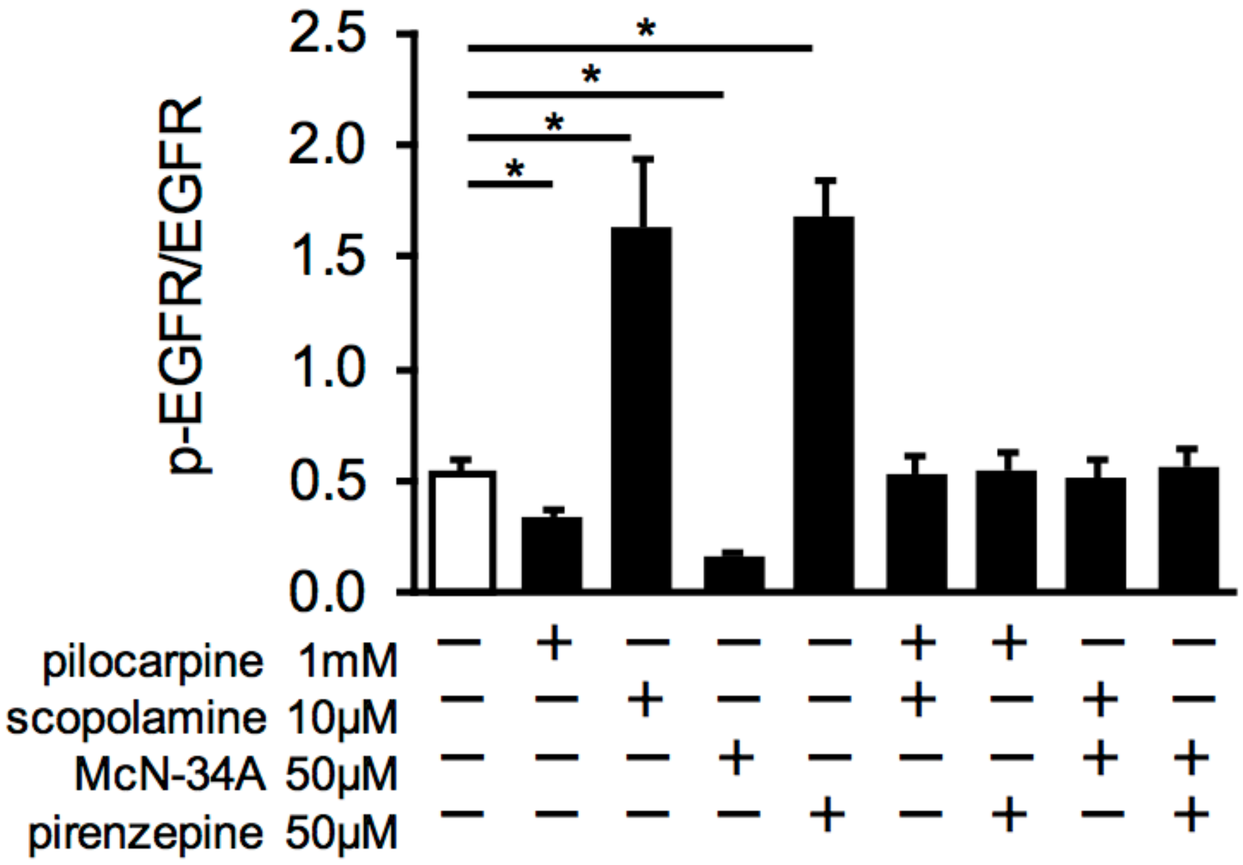

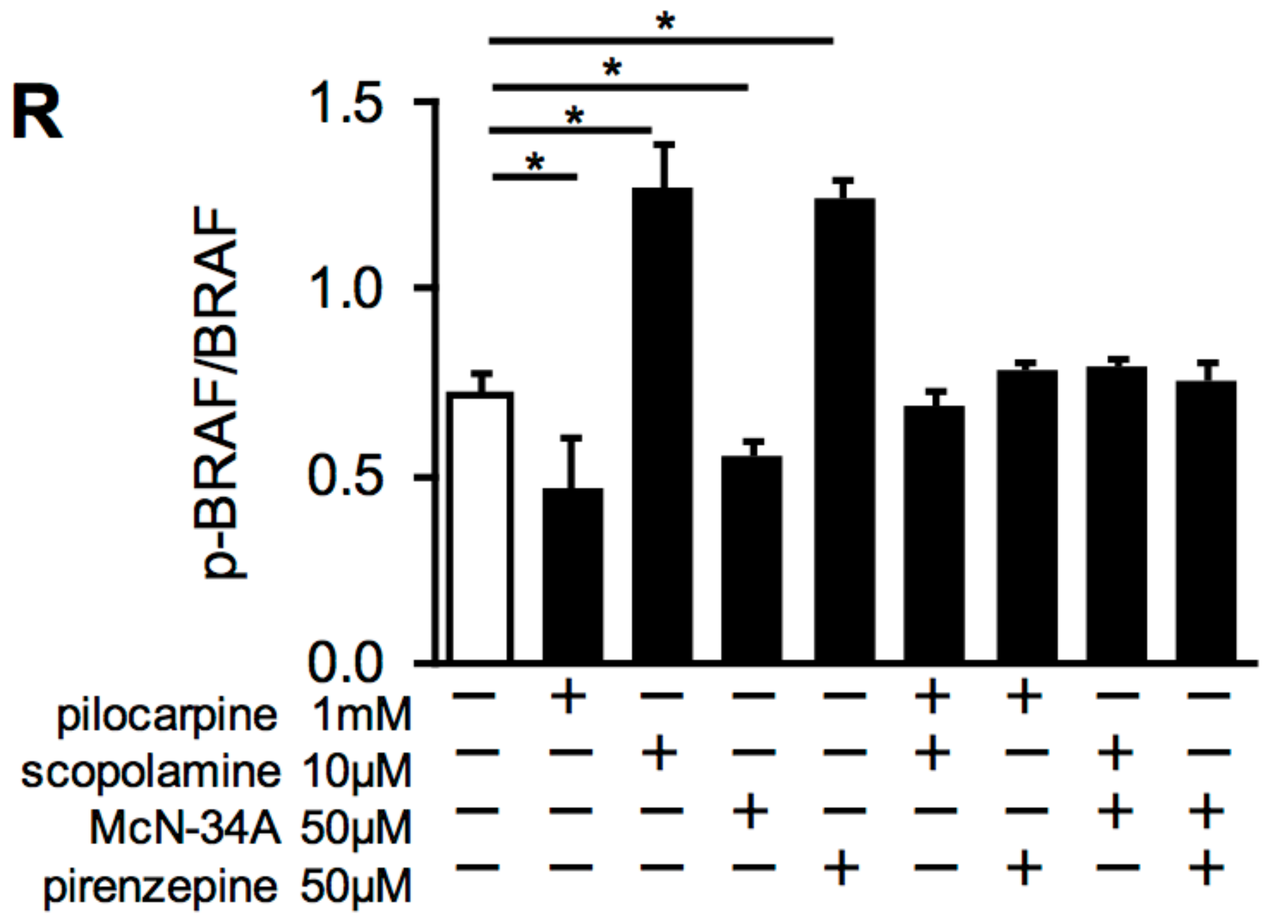

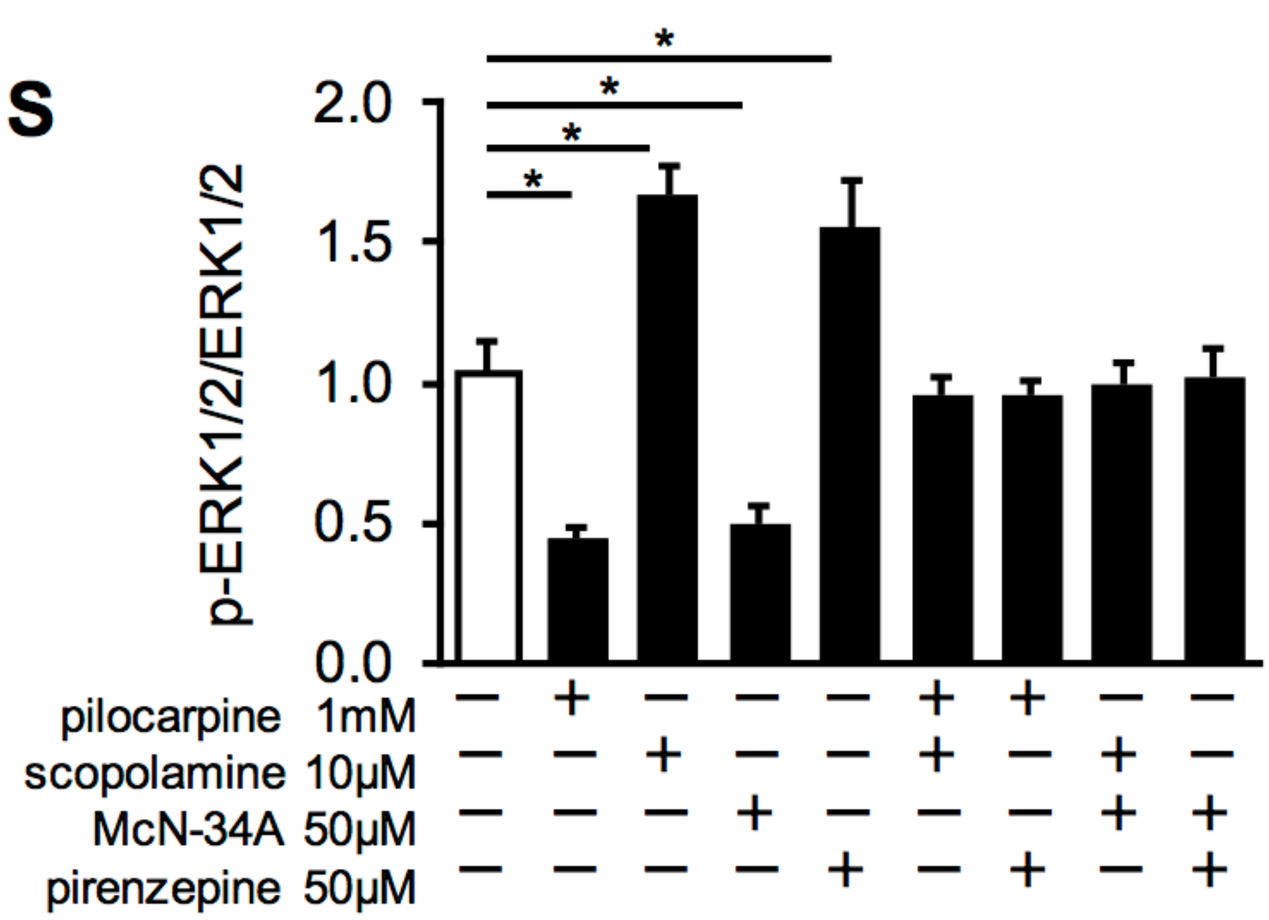

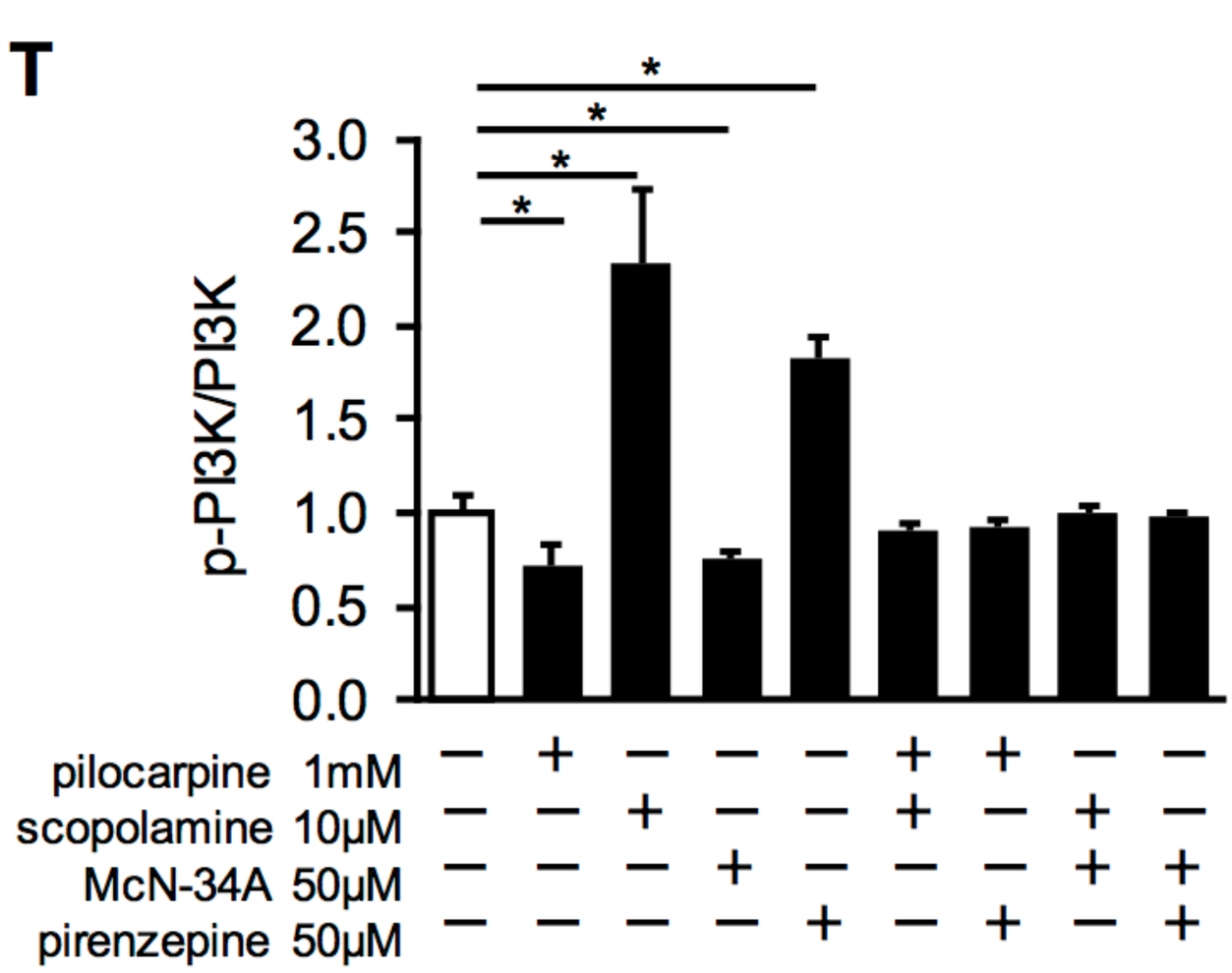

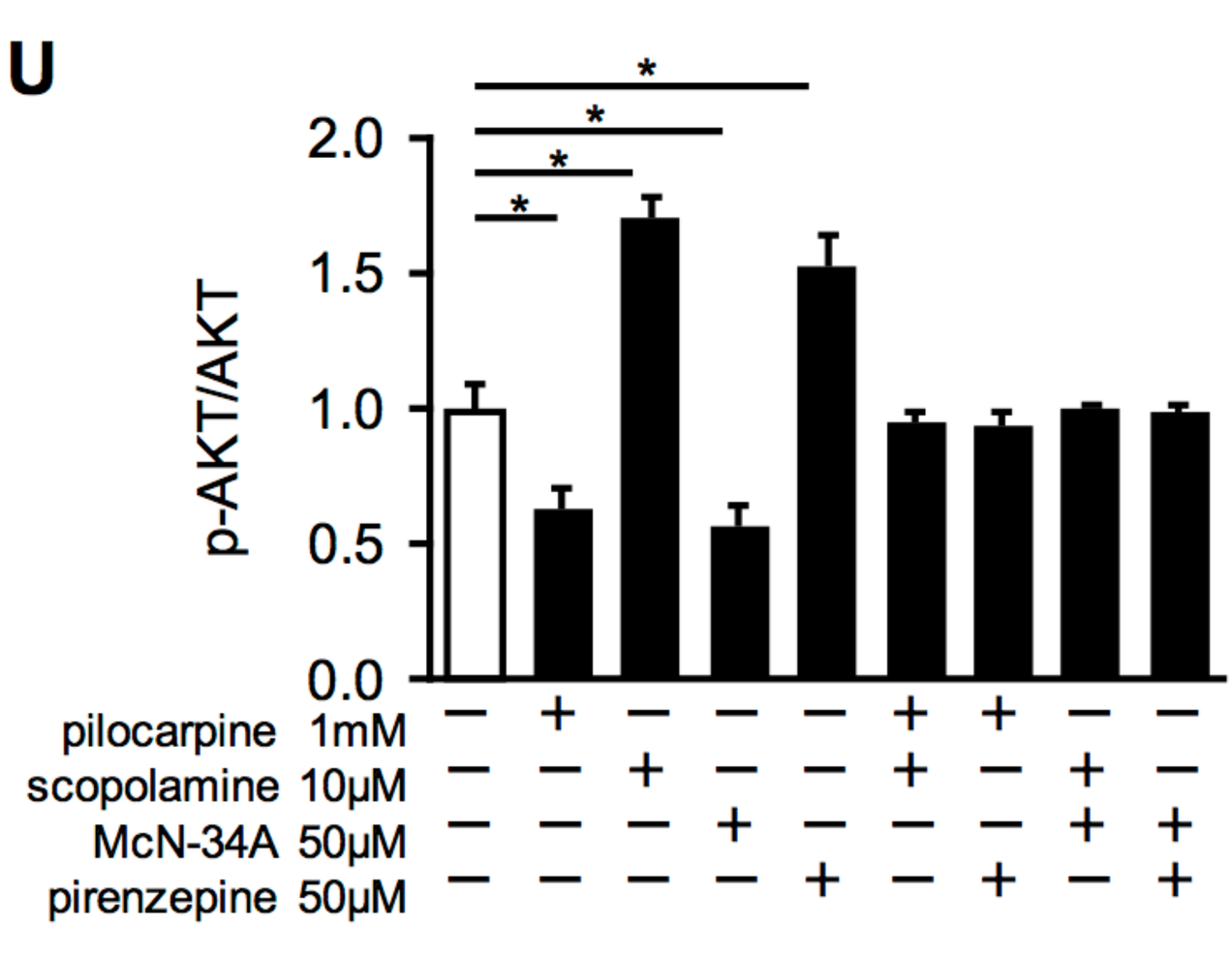

Supplementary Figure 4

A-C. Key KEGG pathways in RNAseq of Panc1 cells with and without treatment with pilocarpine. **A.** Table showing changes in expression of proliferation related genes from RNAseq of Panc1 cells after pilocarpine treatment. Gene symbols in parenthesis indicate how the gene is represented. log_2FC (Fold change) and fold change are for treated versus untreated. **B.** PI3K-AKT pathway. The expression of PIK3CA (PI3K) is downregulated. PIK3CA (PI3K) is activated by both KDR (RTK) and ITGAV (ITGA), both of which are downregulated, which tends to inhibit PI3KCA on a signaling level as well. Inhibition of PI3CA leads to reduction of activation of AKT. Since AKT inhibits p21 (CDKN1A) and p27 (CDKN1B), reduction of activation of AKT leads to an increase in activation of these anti-proliferative genes, thereby slowing the cell cycle. **C.** Classical MAPK signaling pathway. EGFR, NTRK2, and BRAF are all part of a proliferative pathway. Since these genes are downregulated, proliferation is slowed. **D-F.** Representative images of IHC for p-EGFR (**D**), p-PI3K (**E**), and p-ERK1/2 (**F**) in PDAC from KPC mice treated by GEM or GEM+bethanechol. Bar graphs showing quantification of the area stained positive for each protein in PDAC from KPC mice treated with GEM or GEM+bethanechol (n=3, each group). **G.** Representative image from phospho-kinase array. Boxes highlight the relative phosphorylation status of p38a, ERK1/2, EGFR, Akt1/2/3 (S473), Akt 1/2/3 (T308), TOR (S2448) and YES of Panc1 cells without treatment (control) or treated with pilocarpine. **H.** Bar graph showing quantification by densitometry of the phosphorylation status of p38a, ERK1/2, EGFR, Akt1/2/3 (S473), Akt 1/2/3 (T308), TOR (S2448) and YES from the phosphokinase array (n=2, each group). **I.** Western blot analysis of p-EGFR/EGFR and p-ERK1/2/ERK1/2 relative to β-actin after treatment with increasing concentrations of pilocarpine. **J.** Western blot analysis of signaling pathways with or without pilocarpine, scopolamine, McN-34A, and/or pirenzepine treatment of K8282 cells at indicated dosages. **K-O.** Quantification of densitometry of Western blot depicted in **J.** for p-EGFR/EGFR (**K**) p-BRAF/BRAF (**L**), p-ERK1/2/ERK1/2 (**M**), p-PI3K/PI3K (**N**), and p-AKT/AKT (**O**). **P.** Western blot analysis of signaling pathways with or without pilocarpine, scopolamine, McN-34A, and/or pirenzepine treatment of Panc1 cells at indicated dosages. **Q-U.** Quantification of densitometry of Western blot depicted in **P**. for p-EGFR/EGFR (**Q**) p-

BRAF/BRAF (**R**), p-ERK1/2/ERK1/2 (**S**), p-PI3K/PI3K (**T**), and p-AKT/AKT (**U**). Scale bars, 100 μm. Means ± SD. *$p < 0.05$.

Supplementary Figure 5

A

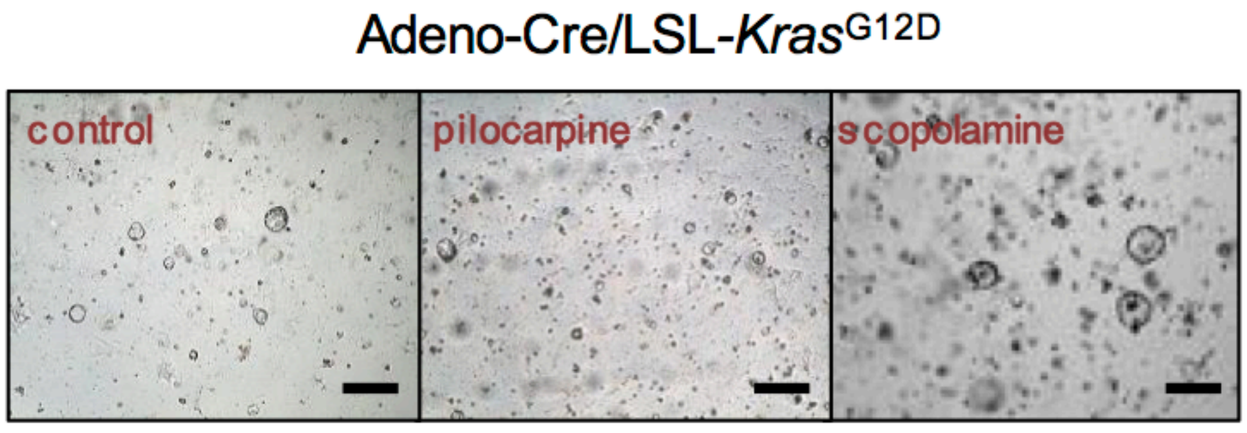

B

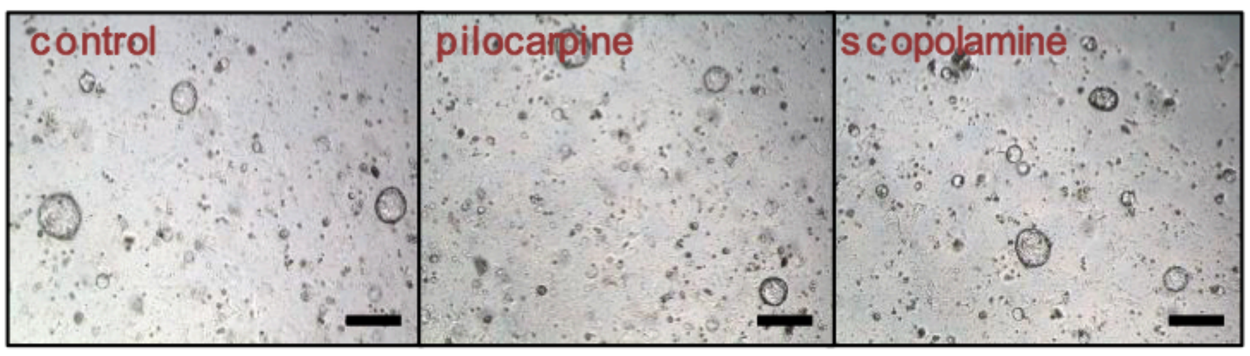

C

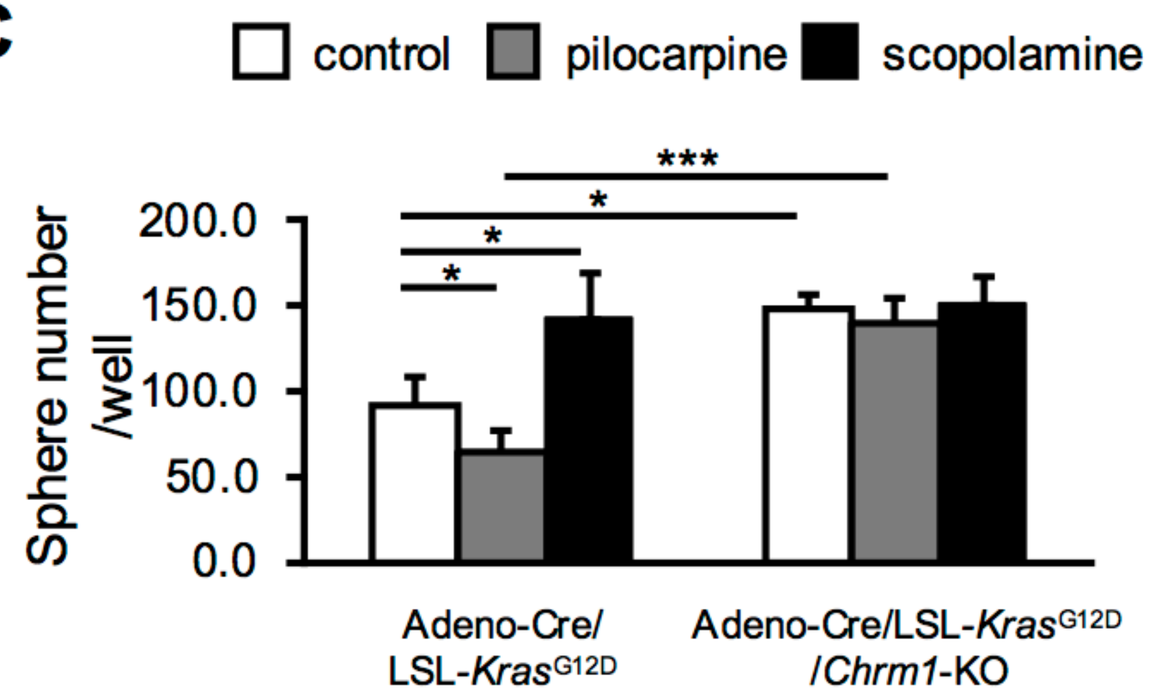

D

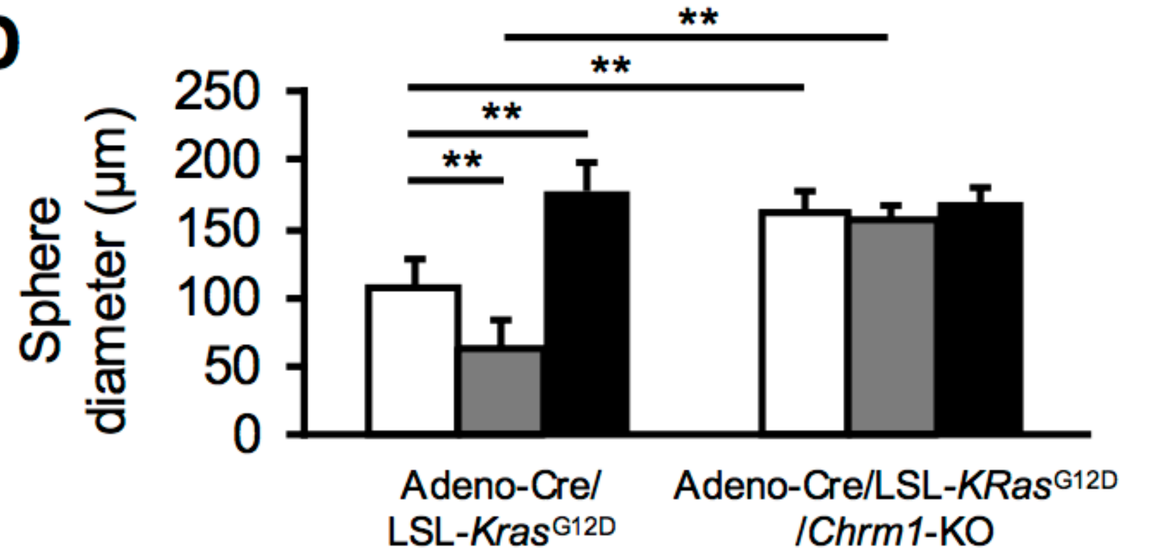

E

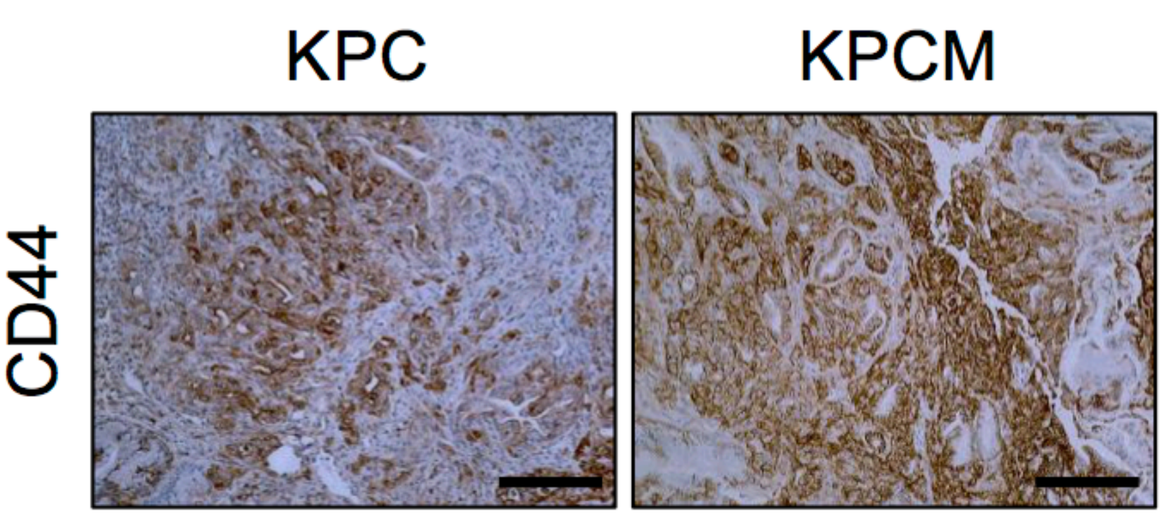

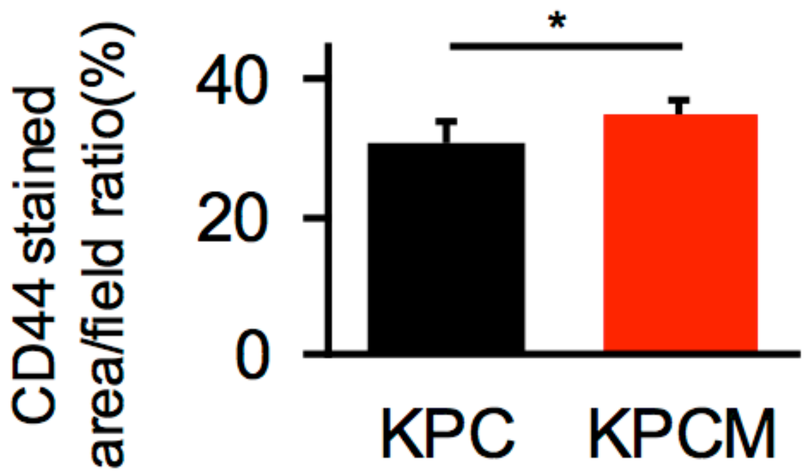

F

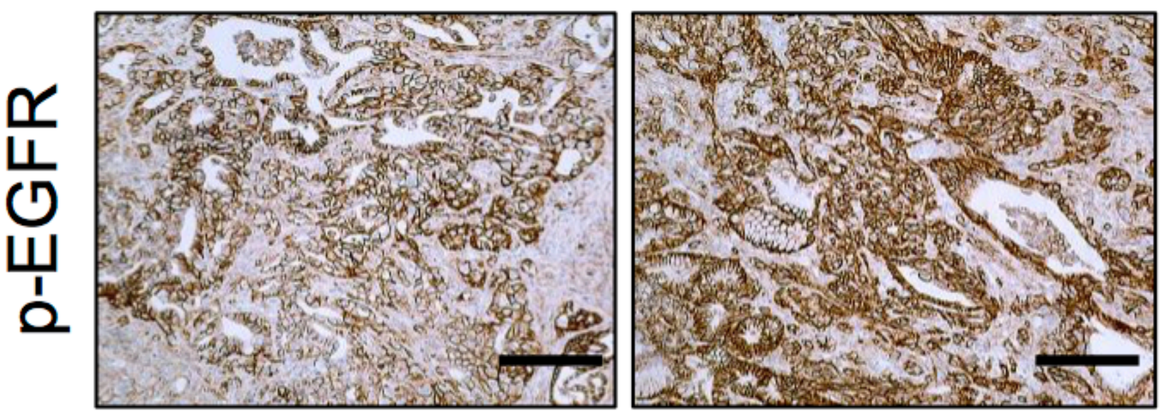

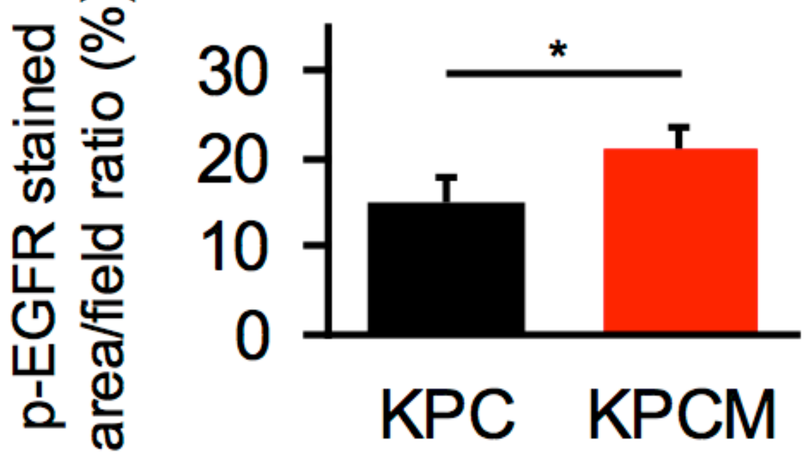

G

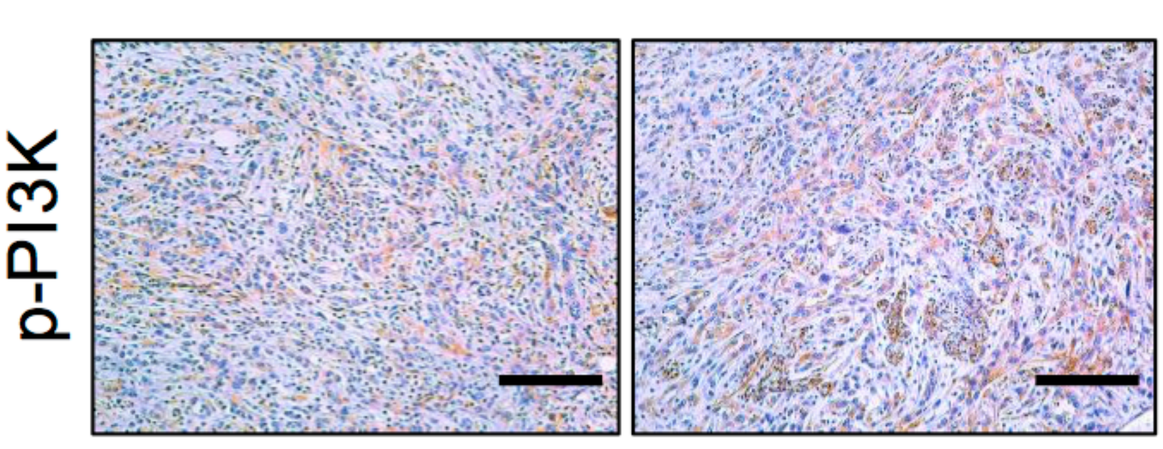

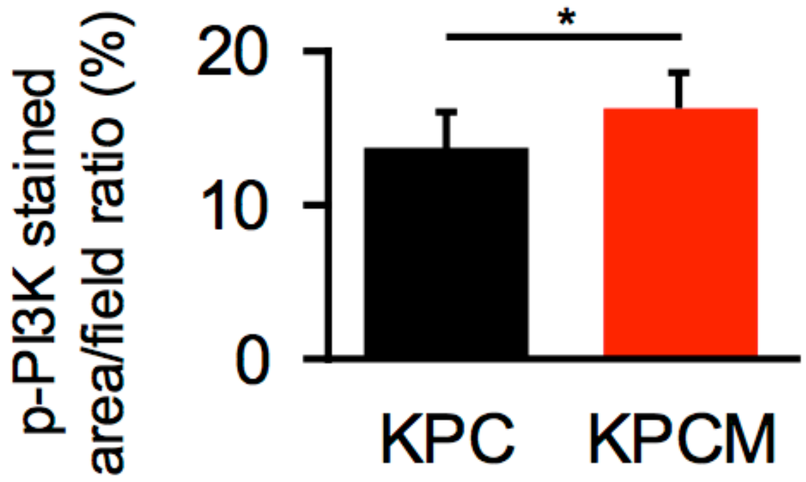

H

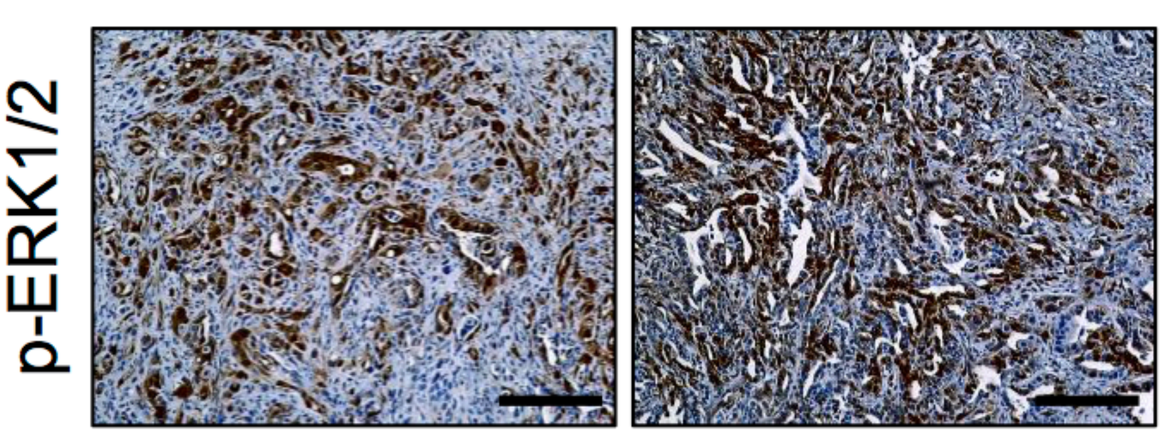

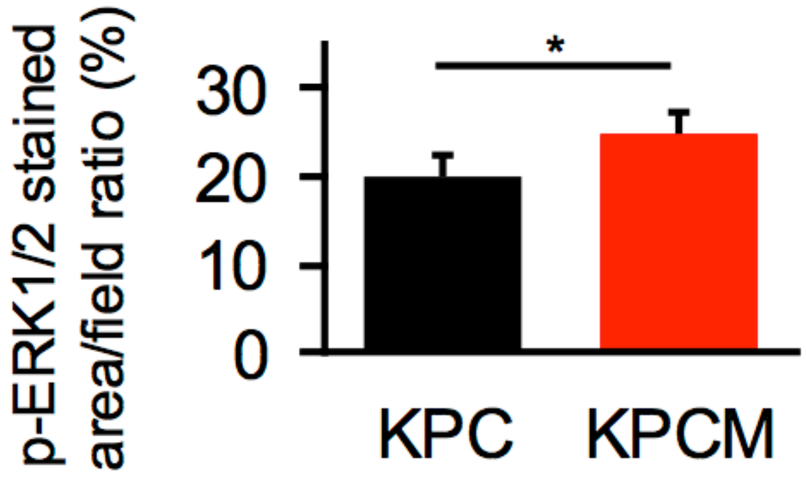

Supplementary Figure 5

A. Representative images of 3D pancreatic spheroid cultures, isolated from LSL-*Kras*$^{+/G12D}$ mice and treated with Adeno-Cre virus alone, Adeno-Cre virus and pilocarpine or Adeno-Cre virus and scopolamine. Spheroid cultures were analyzed at day 5 post isolation**. B.** Representative images of 3D pancreatic spheroid cultures, isolated from LSL-*Kras*$^{+/G12D}$ *Chrm1*-KO mice and treated with Adeno-Cre virus alone, Adeno-Cre virus and pilocarpine or Adeno-Cre virus and scopolamine. Spheroid cultures were analyzed at day 5 post isolation**. C** and **D.** Number (C) and size (D) of pancreatic spheres isolated from LSL-*Kras*$^{+/G12D}$ and LSL-*Kras*$^{+/G12D}$/*Chrm1*-KO mice treated with the drugs indicated. **E-H.** Representative images of pancreatic IHC for CD44 (**E**), p-EGFR (**F**), p-PI3K (**G**), and p-ERK1/2 (**H**) in KPC and KPCM mice. Bar graphs show quantification of each staining in pancreata from KPC and KPCM mice (n=3, each group). Scale bars, 100 μm. Means ± SD. *p < 0.05; **p < 0.01; ***p < 0.001.

Supplementary Figure 6

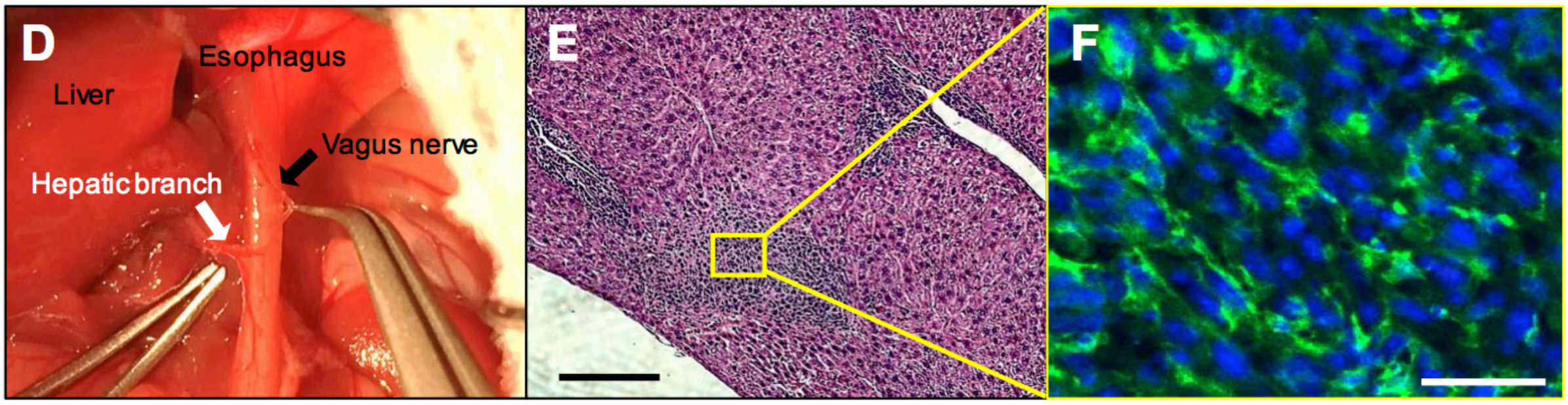

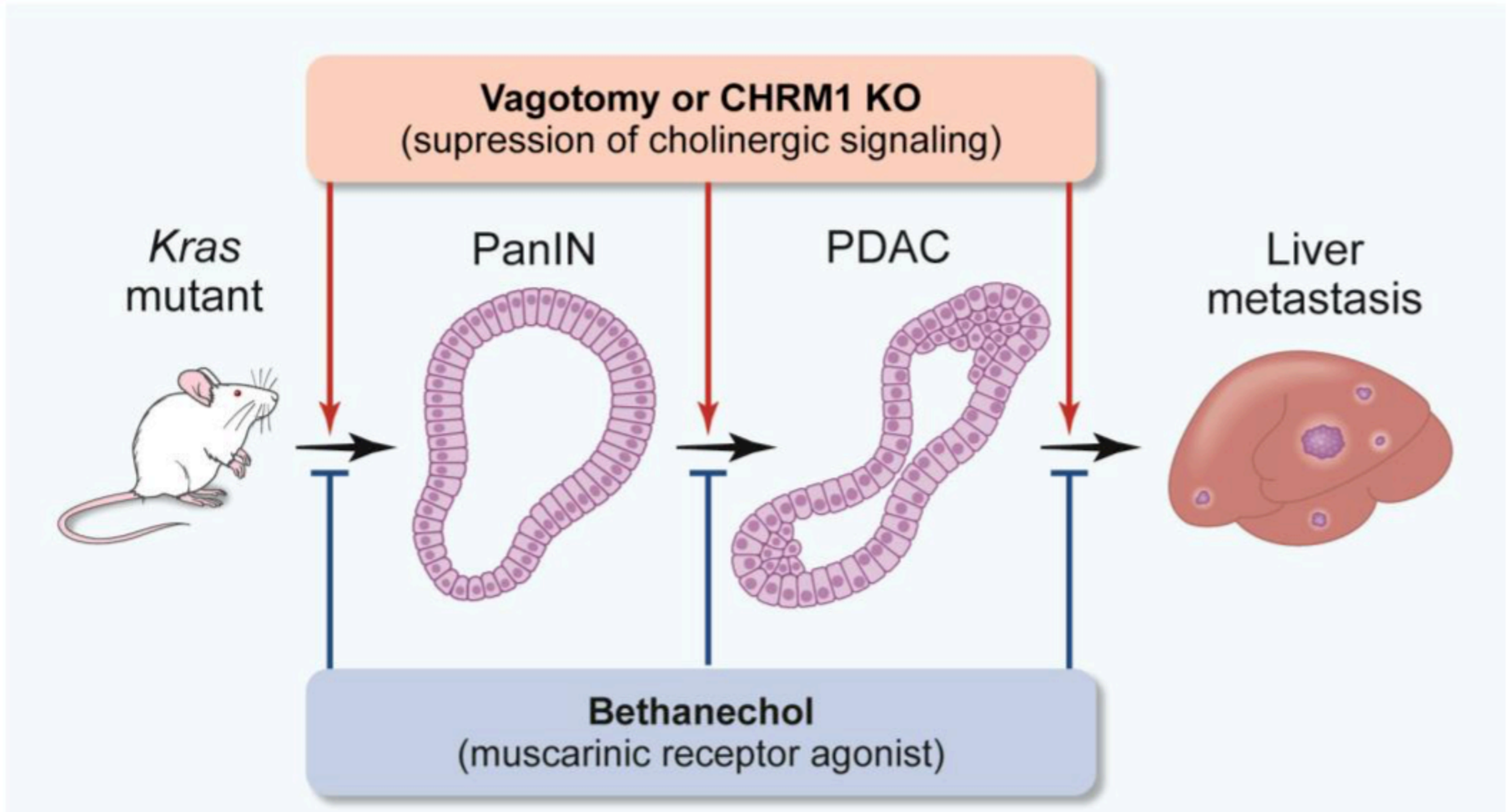

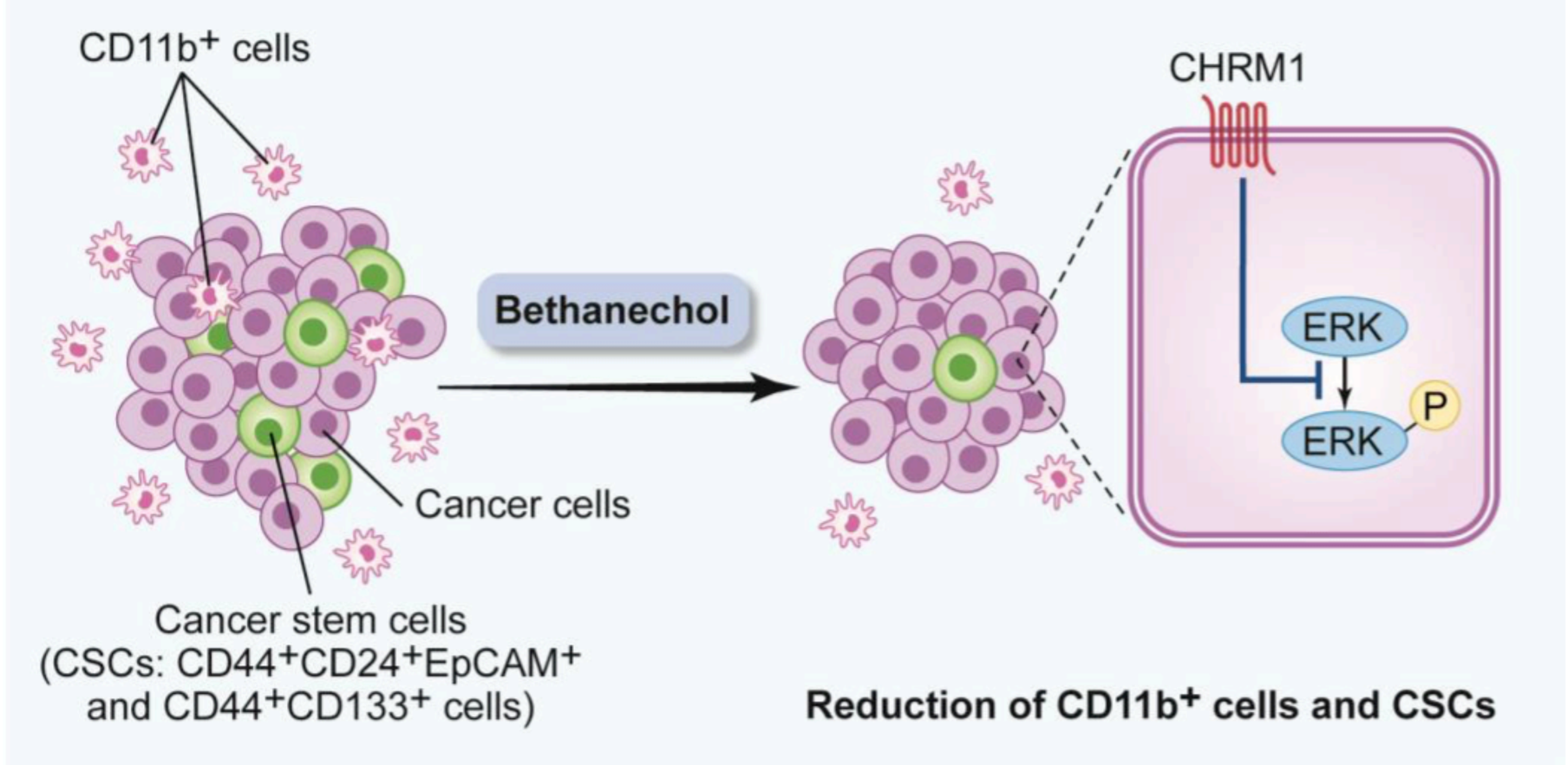

Supplementary Figure 6

A. A left subcostal incision was performed and the spleen was exposed through the incision. **B.** The spleen was divided into upper and lower halves by placing two Horizon medium sized clips in the center of the spleen. Phosphate buffered saline (PBS) was drawn up into a syringe. 100 µl of Panc02 (2×10^6) cells were also drawn up into the same syringe, and the cells were injected slowly into the exposed lower-hemispleen. **C.** Lower hemisplenectomy was performed by dividing the splenic vessels distal to the pancreas. **D.** Anatomical photograph of vagus nerve (black arrow) and hepatic branch (white arrow). **E.** Representative photograph of pancreatic H&E stained section after splenic in injection of Panc02 (2×10^6) cells; Scale bar, 500 µm. **F.** Representative image of pancreatic IHC-F showing GFP-labeled cancer cells in a liver metastasis after splenic injections of 2×10^6 GFP-labeled Panc02 cells; (GFP; green, DAPI; blue). Scale bar, 50 µm. **G.** Graphical abstract showing major findings of the study: subdiaphragmatic vagotomy accelerates pancreatic tumorigenesis in part through an expansion of the cancer stem cell compartment and increased $CD11b^+$ myeloid cells. These effects can be reversed by a muscarinic agonist, (bethanechol), in part through suppression of MAPK signaling, in early stages of tumor growth as well as in more advanced, metastatic disease.

Supplementary Methods

Animal Surgery

All surgical procedures were performed under isoflurane inhalation anesthesia (2-3%), with buprenorphine (0.1 mg/kg subcutaneously) given as postoperative analgesia. Procedures were performed under a binocular surgical microscope with a 3.5× magnification.An upper midline abdominal laparotomy inferior to the xiphoid cartilage was performed for the procedures described, if not stated otherwise. The situs was exposed by using a retraction kit for small animals (Fine Science Tools).

Subdiaphragmatic Bilateral Truncal Vagotomy

The intestine was placed out of the abdominal cavity to the left side wrapped in warm saline moistened gauze. The gastroesophageal junction and the anterior vagus nerve were identified by gently pulling the stomach down and placing some gauze beneath the cardia to lift it up, thereby improving access to the region. At least 5 mm of the visible vagal nerve was isolated. The adventitia surrounding the esophageal muscularis was cut together with the branches of the vagus nerve before the bifurcation of the gastric, hepatic and celiac branches. Then a 2-mm section from the right trunk was removed to prevent reinnervation. The stomach is wrapped in warm saline moistened gauze and placed on the right side of the situs to gain access to the posterior vagus nerve. It was then transected in the same manner as the right side. The stomach was brought back in its anatomical correct position. In sham treated mice both vagus nerves were exposed however not transected.

Pyloroplasty

The bilateral vagotomy was complemented by a pyloroplasty to prevent gastric stasis. The pylorus was identified and a longitudinal transmural incision was made through the pyloric

sphincter. The pyloric wall was then transversely closed using 7-0 PROLENE (ETHICON) in an interrupted pattern. The procedure is also performed in sham treated mice.

Selective hepatic branch vagotomy

The intestine was placed out of the abdominal cavity to the left side wrapped in warm saline moistened gauze. The gastroesophageal junction and the anterior vagus nerve were identified by gently pulling the stomach down and placing some gauze beneath the cardia to lift it up, thereby improving access to the region. The bifurcation of the gastric and hepatic branches was identified and the hepatic branch isolated carefully between forceps. A 2-mm section from the hepatic trunk was transected to prevent reinnervation.

Every procedure ended with a careful examination of the situs to ensure complete hemostasis. Then the intestine was placed back in the abdominal cavity. The incision was closed in a running two-layer fashion using 4-0 vicryl (ETHICON) for muscle layer and clipping (Fine Science Tools) for skin closure.

Liver metastatic procedure and hemi-splenectomy

The liver metastatic model was performed as previously described (1). Briefly, a left subcostal incision was performed, and the spleen was exposed through the incision. The spleen was then divided into upper and lower halves by placing two Horizon medium sized ligation clips (WECK) in the center of the spleen. 150 µl of phosphate buffered saline was drawn up into a 27 G × 5/8” syringe, and 100 µl of Panc02 (2×10^6) cells were also drawn up into the same syringe. Panc02 cells were injected slowly into the exposed lower-hemispleen. Lower hemisplenectomy was performed by ligating splenic vessels and then cutting distally. The incision was closed in a running two-layer fashion using 4-0 vicryl (ETHICON) for muscle layer and clipping (Fine Science Tools) for skin closure.

Quantification of immunohistochemical staining

Ki-67 positive cells were quantified in at least five high power fields from at least 3 mice per group. Total cells per field were counted via morphometric analysis using ImageJ software (NIH) and the ratio of positive cells to total cell number calculated. Stained area was quantified in at least five high power fields from at least 3 mice per group by ImageJ software using color deconvolution mode.

Cell lines and cell culture

Two human PDAC cell lines (Panc1 and MiaPaCa2) and three murine PDAC cell lines (Panc02, K8282 and K2548) were used in this study. All human pancreatic cancer cell lines were purchased from ATCC. Panc02 cells derived from B57BL/6 mice were previously described (2). Murine pancreatic cancer cell lines derived from KPC mice (K2548 and K8282) were provided from Dr. Kenneth P. Olive. RPMI-1640 (Gibco) supplemented with 10% fetal bovine serum (FBS) and Penicillin/Streptomycin (Invitrogen) were used for cell culture. The cell medium was replaced every 48-72 hours. All cultures were maintained in a 5% CO_2 air-humidified atmosphere at 37°C. HPDE (Human Pancreatic Duct Epithelial Cell Line) -Tet-on-*Kras*^{G12D} cell line (3) was cultured with the KSFM medium (Keratinocyte-SFM) with Calcium + 50 μg/ml BPE (Bovine Pituitary Extract: 25 mg 500 ml) + 5 ng/ml EGF (Epidermal Growth Factor; 2.5 μg/500 ml) + 1% FBS. In order to activate the *Kras*-mutant allele in this cell line, doxycycline was added in the media in a concentration of 200 nM. The *Kras*-mutant allele was activated after 12 hours. After 24 hours, media was harvested, and pilocarpine was added in the media with Doxycycline. The plates were analyzed after 72 hours. In order to measure the viability, the CellTiter-Glo Cell Viability Assay (Promega) was used.

Quantitative RT-PCR (qRT-PCR)

Total RNA was extracted from whole pancreas or spleen samples from each animal using RNAlater (Thermo Fisher Scientific) and NucleoSpin RNA (Macherey-Nagel) or the RNAqueous-micro kit (Ambion) and subjected to first-strand complementary DNA synthesis using the Superscript III cDNA Amplification System (Invitrogen) following the manufacturer's instructions. qRT-PCR was performed using a three-step method, an ABI 7300 system and SYBR green (Applied Biosystems). The qRT-PCR primer sequences are listed below. The results were expressed as the copy number of each gene relative to that of GAPDH.

Western blot

To analyze EGFR, MAPK and PI3K-AKT pathways in human and murine pancreatic cancer cell lines, we grew cells in 12-well culture plates to 70% confluency. The medium was changed then to 0.5% FBS medium, the respective drugs added and incubated for an additional 72 hours in a CO_2 incubator (5% CO_2). After removing the medium, cells were washed twice with PBS, and protein extraction was performed on ice using RIPA buffer with protease inhibitor cocktail (Roche) and a phosphatase inhibitor (Roche). Protein samples were subsequently separated by 10% Bis-Tris Gel NuPAGE® electrophoresis using MES SDS Running Buffer (Invitrogen). After transfer to Polyvinylidene difluoride (PVDF) membranes, membranes were blocked with 5% skim milk, and samples were probed with the following primary antibodies: p-EGFR (Y1068) (Cell Signaling), EGFR (Millipore), p-BRAF (Ser445) (Cell Signaling), BRAF (Cell Signaling), p-ERK1/2 (phosphorylated p44/42 MAPK) (Thr202/Tyr204) (Cell Signaling), ERK1/2 (p44/42 MAPK) (Cell Signaling), p-PI3K p85(Tyr458)/p55(tyr199) (Cell Signaling), PI3K (Cell Signaling), p-AKT (T308) (Cell Signaling), AKT (Cell Signaling), and β-actin (Cell Signaling) followed by horseradish peroxidase–coupled secondary antibody.

Immunoreactive bands were visualized using Pierce™ ECL Western Blot Substrate (Thermo Fisher Scientific) and bands were quantified with ImageJ software.

MTT assay and Soft agar assay

Cell proliferation in each cell line was assessed with a 3-(4,5-dimethylthiazol-2yl)-2,5-diphenyltetrazolium bromide (MTT) assay kit (Sigma) in accordance with manufacturer's instructions. We grew 3×10^3 cells in 96-well plate to 70% confluency, changed the media to 0.5% FBS medium, added the respective drugs and incubated them for an additional 72 hours in a CO_2 incubator (5% CO_2). Treated cells were rinsed twice with PBS, incubated in MTT solution (5 mg/ml in PBS) for 4 hours at 37 °C, and 100 µl DMSO was added to each well. The absorbance of each well was measured at 570 nm using a Tilter-Tech 96-well multiscanner (Becton Dickinson). The relative number of viable cells compared with the number of cells without drug treatment was expressed as percent cell viability using the following formula: cell viability (%) = A_{570} of treated cells/A_{570} of untreated cells.

Soft agar assay was employed to identify the ability of Panc1 cells and K8282 cells to grow as anchorage-independent colonies. Briefly, 2 ml of 0.6 % low-melting point agarose (Lonza) in RPMI-1640 medium containing 10 % FBS was poured into a 6-well plate and allowed to solidify at room temperature. After solidification, 500 cells were suspended in 1 ml of 0.35 % low-melting point agarose in the same medium and then plated on top of the base layer (three wells per group). The cells were cultured for 18 days. Colonies with at least 50 cells were counted using a microscope at 100×magnification, and the number of colonies in soft agar (five fields per well) was quantified.

Flow cytometry

We grew Panc1, K2548 and K8282 cells in 6-well plate to 70% confluency, changed the media to 0.5% FBS medium, added pilocarpine and incubated them for an additional 72

hours in a CO_2 incubator (5% CO_2). Subsequently, cells were kept on ice in blocking solution (PBS pH 7.2 containing 3% bovine serum albumin, 2 mM EDTA) for 20 minutes. Cells were then stained with a PE-conjugated antibody against CD24, a FITC-conjugated antibody against CD44, an APC-conjugated antibody against CD326 and a PE-Cy7-conjugated antibody against CD133 (all 1:100 in blocking solution, Biolegend) on ice for 30 minutes. The cells were then washed, reconstituted in sorting buffer (PBS pH 7.2 containing 0.5% bovine serum albumin, 2 mM EDTA) + DAPI and analyzed using a BD LSRFortessa.

For *in vivo* analysis, we treated KPC mice bearing 3-5 mm tumors with gemcitabine with or without bethanochol for two weeks and then sacrificed them. Tumor tissue was chopped into small pieces and digested in 1 mg/ml collagenase-V (Sigma-Aldrich) at 37 C° for 2 hours. Following multiple washes with PBS supplemented with 2% fetal bovine serum (FBS), collagenase-digested pancreatic tissue was spun down and further digested with 0.05% trypsin-EDTA (Gibco). Red blood cells were lysed (ACK Lysing Buffer) before passing through a 40 μm nylon mesh. After multiple washes, white blood cells were removed with Lineage Depletion Kit (Miltenyl Biotec). Collected single cells were stained and analyzed as described previously in this section. In immune cell analysis *in vivo*, spleens were harvested and kept on ice. Spleens were mechanically dissociated thoroughly and passed through 40 μm nylon mesh. Following multiple washes using PBS with 2% FBS, red blood cells were Lysed by 1ml ACK Lysing Buffer on ice for 3 minutes. After wash, these single cells were incubated with an APC-conjugated antibody against CD3, a PE-Cy7-conjugated antibody against CD45, a PE-conjugated antibody against B220, an APC-conjugated antibody against CD11b, and a FITC-conjugated antibody against F4/80 (all 1:100 in blocking solution, Biolegend) on ice for 20 minutes. The cells were then washed, reconstituted in sorting buffer (PBS with 2% FBS) with DAPI (1:5000) and analyzed as described above. The graphs of gate were created by FlowJo v10 software

(Tree Star, Inc.).

Generation of Panc02 cells stably expressing GFP protein

Panc02 cells stably expressing GFP proteins (Panc02-GFP) were generated as follows. Parental Panc02 cells were transduced with 5×10^6 IFU Lentivirus particles containing GFP vectors under the control of suCMV promoter (GenTarget Inc.). Transduced cells were incubated with puromycin (2 μg/ml) for 1 week to select GFP-positive cells. Strong GFP-expressing cells were pooled and further sorted by BD FACSAria™ II. Afterwards they were cultured in the complete medium containing puromycin. Stable Panc02-GFP cells were maintained by puromycin at 0.5 μg/ml prior to intra-splenic injection.

Enzyme-linked Immunosorbent assay (ELISA)

ELISA for murine TNF-α (R&D) was performed according to manufacturer's protocols.

Phospho-kinase Assay

For phosphokinase profiling, Panc1 cells were seeded at 60-70% confluency, starved in low serum medium (0.5% FBS) for 4hrs and then treated with fresh medium (0.5% FBS) containing either PBS or pilocarpine (100 μM) for 15 min. Cells were then lysed and the proteome profiler human phosphokinase profiling was performed following the manufacturer's protocols (R&D Systems).

RNAseq Analysis

Sequenced reads were mapped to the NCBI annotated genes of the mm9 assembly of the mouse genome with BowTie2 and TopHat 2.0.4 (4,5). Reads were counted with HTSeq. The full RNA-seq data have been deposited in the Gene Expression Omnibus (https://www.ncbi.nlm.nih.gov/geo/) under the accession Code GEO: GSE102880.

Samples were normalized with the TMM algorithm. The statistical significance of differential expression was estimated with weighted Limma-Voom (6) which runs under Bioconductor/R (7 & https://www.R-project.org/). Significantly differentially expressed genes (8) ≤ 0.05 and absolute value of log2 fold change ≥ 0.6, were analyzed further. First, a screen in terms of Gene Ontology (9) categories for consistency with phenotype was performed. Genes were retained which either:

1. Upregulated and negatively regulate the cell cycle (GO:0045786).
2. Downregulated and positively regulate the cell cycle (GO:0045786).
3. Upregulated and positively regulate the apoptotic process (GO:0043065).
4. Downregulated and negatively regulate the apoptotic process (GO:0043066).

57 genes fulfilled these requirements. These genes were analyzed further in terms of KEGG pathways (10) with iPathwayGuide (11).

Statistical Analysis

The means of two groups were compared using Student's t-test or Mann-Whitney U-test. Kaplan-Meier survival curves were analyzed by log-lank test. Multi-group comparisons were performed using one-way ANOVA test followed by Kruskal-Wallis test. P values < 0.05 were considered to indicate statistical significance. All statistical analyses were performed using Prism 7 (GraphPad Software, Inc.).

List of qRT-PCR primers (mouse) used in this study

Gene	Forward (5'->3')	Reverse (5'->3')
Chrm1	CAGAAGTGGTGATCAAGATGCCTAT	GAGCTTTTGGGAGGCTGCTT
Chrm2	TGGAGCACAACAAGATCCAGAAT	CCCCTGAACGCAGTTTTCA
Chrm3	CCAGTTGGTGTGTTCTTCCTT	AGGAAGAGCTGATGTTGGGA
Chrm4	GTGACTGCCATCGAGATCGTAC	CAAACTTTCGGGCCACATTG
Chrm5	GGCCCAGAGAGAACGGAAC	TTCCCGTTGTTGAGGTGCTT
Tnfa	CCCTCACACTCAGATCATCTTCT	GCTACGACGTGGGCTACAG
Gapdh	TCATTGTCATACCAGGAAATGAG	AGAAACCTGCCAAGTATGATGAC

List of qRT-PCR primers (human) used in this study

Gene	Forward (5'->3')	Reverse (5'->3')
CHRM1	TTCCTCAGGGGAAAGTCATC	GTGTTTGGGTCCCTGGAGA
CHRM2	TGCGTTCTCTAATCAGTAGCCA	CTTCAAGCCTCCACCACCTC
CHRM3	GGCCTGTGCCGATCTGATTAT	CGGCCTCGTGATGGAAAAG
CHRM4	AGATTGTGACGAAGCAGACAGGCA	TTTAAAGGTGGCGTTGCACAGAGC
CHRM5	GACCAACAATGGCTGTCACAAGGT	TCTGTTGCAGAGGGCATAGCAGAT
GAPDH	CCCCATGGTGTCTGAGCG	CGACAGTCAGCCGCATCTT

Supplementary References

1. Soares KC, Foley K, Olino K, Leubner A, Mayo SC, Jain A, et al. A preclinical murine model of hepatic metastases. J Vis Exp. 2014;:51677–7.
2. Corbett TH, Roberts BJ, Leopold WR, Peckham JC, Wilkoff LJ, Griswold DP, et al. Induction and chemotherapeutic response of two transplantable ductal adenocarcinomas of the pancreas in C57BL/6 mice. Cancer Res. 1984;44:717–26.
3. Ouyang H, Mou L, Luk C, Liu N, Karaskova J, Squire J, et al. Immortal human pancreatic duct epithelial cell lines with near normal genotype and phenotype. Am J Pathol. 2000;157:1623–31.
4. Langmead B, Salzberg SL. Fast gapped-read alignment with Bowtie 2. Nat Methods. 2012;9:357–9.
5. Kim D, Pertea G, Trapnell C, Pimentel H, Kelley R, Salzberg SL. TopHat2: accurate alignment of transcriptomes in the presence of insertions, deletions and gene fusions. Genome Biol. BioMed Central; 2013;14:R36.
6. Law CW, Chen Y, Shi W, Smyth GK. voom: Precision weights unlock linear model analysis tools for RNA-seq read counts. Genome Biol. 2014;15:R29.
7. Gentleman RC, Carey VJ, Bates DM, Bolstad B, Dettling M, Dudoit S, et al. Bioconductor: open software development for computational biology and bioinformatics. Genome Biol. 2004;5:R80.
8. Benjamini Y, online YHFTA, 1995. Controlling the false discovery rate: a practical and powerful approach to multiple testing JR Stat Soc B 57: 289–300.
9. Kanehisa M, Goto S, Kawashima S, Okuno Y, Hattori M. The KEGG resource for deciphering the genome. Nucleic Acids Research. 2004;32:D277–80.

10. Draghici S, Khatri P, Tarca AL, Amin K, Done A, Voichita C, et al. A systems biology approach for pathway level analysis. Genome Research. 2007;17:1537–45.
11. Tarca AL, Draghici S, Khatri P, Hassan SS, Mittal P, Kim JS, et al. A novel signaling pathway impact analysis. Bioinformatics. 2008;25:75–82.